

The re-description of *Liaoningotitan sinensis* Zhou et al., 2018

Bingqing Shan

Department of Paleontology College, Shenyang Normal University, Shenyang, Liaoning Province, China

ABSTRACT

Liaoningotitan sinensis is one of three sauropod species found in the Jehol Biota. *Liaoningotitan sinensis* is from the Lower Cretaceous Yixian Formation in Liaoning, China. The discovery of *Liaoningotitan sinensis* was an important breakthrough for researching the diversity of giant herbivorous animals in the Jehol Biota. However, the research and analysis of *Liaoningotitan sinensis* are not yet complete. This study presents a comprehensive research and analysis of *Liaoningotitan sinensis* holotype. First, the skull, vertebrae, pelvic girdle, and appendicular elements of *Liaoningotitan sinensis* holotype were carefully reexamined, leading to the discovery of mosaic evolution occurring in the skull and the identification of one new autapomorphy of humerus of *Liaoningotitan sinensis*: the attachment point of coracobrachialis muscle on the anterior surface of the proximal end of the humerus is flat. Second, the characteristics of the *Liaoningotitan sinensis* holotype and other well-preserved sauropod dinosaurs were used to reconstruct the skull of *Liaoningotitan sinensis*. Next, *Euhelopus zdanskyi* was used to reconstruct the body type of *Liaoningotitan sinensis* holotype, the result indicating that *Liaoningotitan sinensis* was approximately 10 m in length. Finally, TNT software was utilized to analyze the phylogenetic position of *Liaoningotitan sinensis*, with the result indicating that *Liaoningotitan sinensis* can be classified into the Euhelopodidae.

Subjects Evolutionary Studies, Paleontology, Zoology

Keywords Sauropod, Dinosaur, Titanosauriformes, Euhelopodidae, Eusauropoda, Jehol biota, Liaoningotitan, Neosauropoda, Titanosauria, Diamantinasaurus

INTRODUCTION

Titanosauriform is a group of widely distributed sauropod dinosaurs that flourished during the Cretaceous period. Extensive fossil evidence has revealed they inhabited all continents, with large populations in East Asia and South America (*Gorscak & O'Connor, 2016*). The majority of Titanosauriformes in East Asia have been discovered in China. Thirty-two Titanosauriformes species have been named in this country hitherto (*Xu, You & Mo, 2021; Han et al., 2024*), as shown in [Table 1](#). The western part of Liaoning province in China was a distribution region in the Jehol Biota during the Early Cretaceous period. The Jehol Biota is notable for its feathered non-avian theropod dinosaurs, early avians, pterosaurs, and early mammals (*Zhang, 2020*). However, only three Titanosauriformes have been discovered in the Jehol Biota: *Dongbeititan dongi*, *Liaoningotitan sinensis*, and *Ruixinia zhangii* (*Wang et al., 2007; Zhou et al., 2018; Mo et al., 2022*).

Submitted 28 August 2024
Accepted 20 February 2025
Published 11 March 2025

Corresponding author
Bingqing Shan, 1790124692@qq.com

Academic editor
Viktor Brygadyrenko

Additional Information and
Declarations can be found on
page 24

DOI [10.7717/peerj.19154](https://doi.org/10.7717/peerj.19154)

© Copyright
2025 Shan

Distributed under
Creative Commons CC-BY 4.0

OPEN ACCESS

Table 1 Titanosauriformes in China (adapted from *Han et al., 2024*).

| Taxon | Location and formation | Classification | References |
|---|---|-------------------------------|--------------------------------------|
| <i>Liaoningotitan sinensis</i> | Beipiao County Liaoning Province Yixian Formation Early Cretaceous | Euhelopodidae (This study) | <i>Zhou et al. (2018)</i> |
| <i>Dongbeitian dongi</i> | Beipiao County Liaoning Province Yixian Formation Early Cretaceous | Somphospondyli | <i>Wang et al. (2007)</i> |
| <i>Ruixinia zhangi</i> | Beipiao County Liaoning Province Yixian Formation Early Cretaceous | Titanosauria | <i>Mo et al. (2022)</i> |
| <i>Borealosaurus wimani</i> | Beipiao County Liaoning Province Sunjiawan Formation Late Cretaceous | Saltosauridae | <i>You et al. (2004)</i> |
| <i>Jiutaisaurus xidiensis</i> | Changchun city Jilin Province Quantou Formation Late Cretaceous | Titanosauriformes | <i>Wu (2006)</i> |
| <i>Huabeisaurus allocotus</i> | Tianzhen County Shanxi Province Huiquanpu Formation Late Cretaceous | Non-Lithostrotia Titanosauria | <i>Pang & Cheng (2000)</i> |
| <i>Euhelopus zdanskyi</i> | Mengyin City Shandong Province Mengyin Formation Early Cretaceous | Euhelopodidae | <i>Poropat & Benjamin (2013)</i> |
| <i>Zhuchengtitan zangjiazhuangensis</i> | Zhucheng City Shandong Province Wangshi Group Late Cretaceous | Saltosauridae | <i>Mo et al. (2017)</i> |
| <i>Sonidosaurus saihangaobiensis</i> | Erenhot City Inner Mongolia Autonomous Region Erlian Formation Late Cretaceous | Titanosauria | <i>Xu et al. (2006)</i> |
| <i>Mongolosaurus haplodon</i> | Erenhot City Inner Mongolia Autonomous Region On gong Formation Early Cretaceous | Titanosauria | <i>Mannion (2011)</i> |
| <i>Gobititan shenzhouensis</i> | Subei County Gansu Province Xinminpu Group Early Cretaceous | Euhelopodidae | <i>You, Tang & Luo (2003)</i> |
| <i>Yongjinglong datangi</i> | Yongjing County Gansu Province Hekou Group Early Cretaceous | Euhelopodidae | <i>Li et al. (2014)</i> |

Table 1 (continued)

| Taxon | Location and formation | Classification | References |
|---------------------------------------|--|-------------------------------|-------------------------------------|
| <i>Daxiatitan binglingi</i> | Linxia Autonomous District Gansu Province Hekou Group Early Cretaceous | Titanosauria | You et al. (2008) |
| <i>Qiaowanlong kangxii</i> | Subei County Gansu Province Xinminpu Group Early Cretaceous | Euhelopodidae | Li & You (2009) |
| <i>Huanghetitan liujiaxiaensis</i> | Linxia Autonomous District Gansu Province Hekou Group Early Cretaceous | Somphospondyli | You et al. (2006) |
| <i>Hamititan xinjiangensis</i> | Hami City Xinjiang Autonomous Region Shengjinkou Formation Early Cretaceous | Somphospondyli | Wang et al. (2021) |
| <i>Fushanosaurus qitaiensis</i> | Qitai County Xinjiang Autonomous Region Shishigou Formation Late Jurassic | Titanosauriformes | Wang et al. (2019) |
| <i>Silutitan sinensis</i> | Hami City Xinjiang Autonomous Region ShengjinKou Formation Early Cretaceous | Euhelopodidae | Wang et al. (2021) |
| <i>Ruyangosaurus giganteus</i> | Ruyang County Henan Province Haoling Formation Early Cretaceous | Somphospondyli | Lü et al. (2014) |
| <i>Huanghetitan ruyangensis</i> | Ruyang County Henan Province Haoling Formation Early Cretaceous | Somphospondyli | Lü et al. (2007) |
| <i>Xianshanosaurus shijiagouensis</i> | Ruyang County Henan Province Haoling Formation Early Cretaceous | Lithostrotia | Lü et al. (2009) |
| <i>Yunmenglong ruyangensis</i> | Ruyang County Henan Province Haoling Formation Early Cretaceous | Euhelopodidae | Lü et al. (2013a) |
| <i>Baotianmansaurus henanensis</i> | Neixiang County Henan Province Gaogou Formation Late Cretaceous | Non-Lithostrotia Titanosauria | Zhang et al. (2009) |
| <i>Qinlingosaurus luonanensis</i> | Luonan County Shaanxi Province Shanyang Formation Late Cretaceous | Titanosauria | Xue et al. (1996) |

(Continued)

Table 1 (continued)

| Taxon | Location and formation | Classification | References |
|-------------------------------------|--|-------------------------------|---|
| <i>Dongyangosaurus sinensis</i> | Zhejiang Province Fangyan Formation Late Cretaceous | Non-Lithostrotia Titanosauria | Lü et al. (2008) |
| <i>Jiangshanosaurus lixianensis</i> | Zhejiang Province Jinhua Formation Early Cretaceous | Somphospondyli | Tang et al. (2001) |
| <i>Gandititan cavocadatus</i> | Ganzhou City Jiangxi Province Zhoutian Formation Late Cretaceous | Titanosauria | Han et al. (2024) |
| <i>Jiangxititan ganzhouensis</i> | Ganzhou City Jiangxi Province Nanxiong Formation Late Cretaceous | Titanosauria | Mo et al. (2023) |
| <i>Gannansaurus sinensis</i> | Ganzhou City Jiangxi Province Nanxiong Formation Late Cretaceous | Euhelopodidae | Lü et al. (2013b) |
| <i>Fusuisaurus zhaoi</i> | Fusui County Guangxi Autonomous Region Napai Formation Early Cretaceous | Titanosauriformes | Mo et al. (2006) |
| <i>Qingxiusaurus youjiangensis</i> | Nanning City Guangxi Autonomous Region Red bed Late Cretaceous | Titanosauria | Mo et al. (2008) |
| <i>Liubangosaurus hei</i> | Fusui County Guangxi Autonomous Region Napai Formation Early Cretaceous | Titanosauriformes | Mo, Xu & Buffetaut (2010) |

Due to the scarcity of well-preserved Titanosauriform specimens, the identification and phylogenetic analysis of Titanosauriformes are hampered. Fortunately, compared to most other Titanosauriformes, *Liaoningotitan sinensis* is well-preserved, particularly its skull. The type and structure of the skull reveal characteristics of the transitional phase from early-diverging to late-diverging Titanosauriformes. *Liaoningotitan* holotype individuals were first described in the article published in 2018, However, the original research article does not conduct comprehensive research, especially in appendicular elements and dorsal vertebrae. Therefore, it is necessary to assess the osteology of the holotype of *Liaoningotitan sinensis* again.

METHODS

The holotype of *Liaoningotitan sinensis* is housed in the Paleontological Museum of Liaoning (PMOL), Shenyang Normal University in Shenyang City, Liaoning Province, China. It was unearthed in the Xiaobeigou Village, Shangyuan Town, Beipiao City, Chaoyang City of Liaoning Province (Catalogue number: PMOL-AD00112) ([Fig. 1](#)). This holotype includes a skull with mandibula, vertebrae, appendicular elements, and pelvic girdle. The original research article published in 2018 described and conducted a

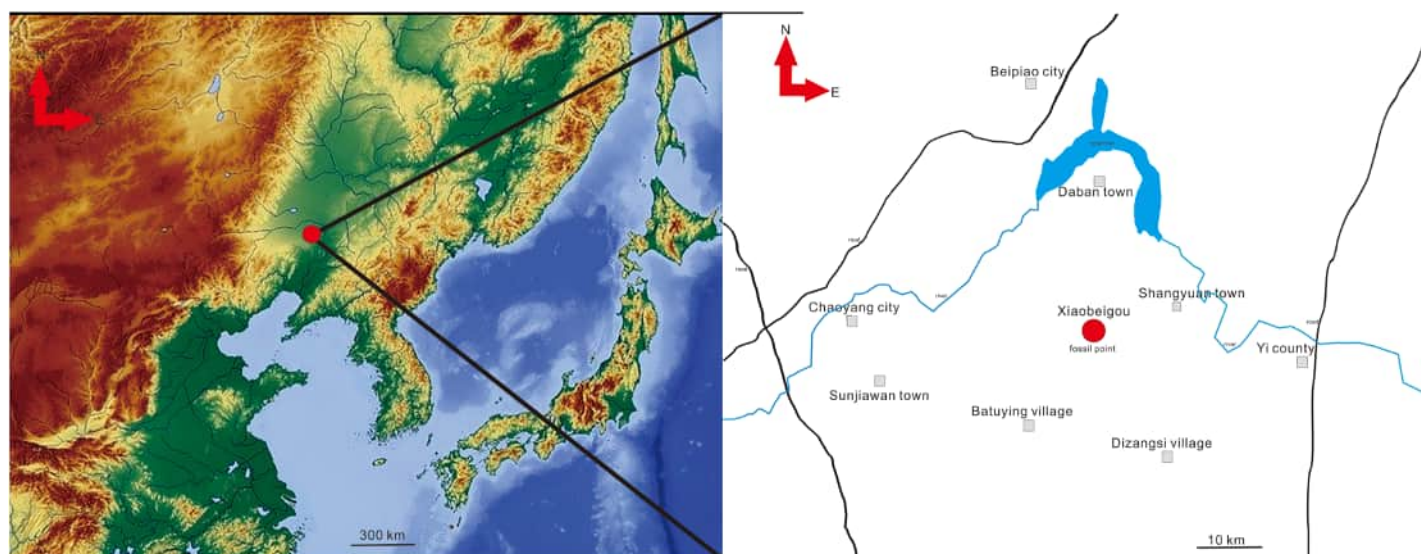



Figure 1 Geographic provenance of *Liaoningotitan sinensis* Zhou et al. (2018). Holotype locality of *Liaoningotitan sinensis* (red point) in Xiaobeigou Village, Shangyuan Town, Beipiao City, Chaoyang City, Liaoning Province, China; Left map copyright: <https://pixabay.com/>; Right map copyright: <https://map.tianditu.gov.cn/>. Full-size  DOI: 10.7717/peerj.19154/fig-1

phylogenetic analysis of *Liaoningotitan sinensis* holotype. However, the article has not described individuals of the *Liaoningotitan* holotype deeply, some characteristics were ignored, such as some characteristics in appendicular elements and dorsal vertebrae. The matrix used in the article was already obsoleted in 2024. Therefore, the holotype specimen of *Liaoningotitan sinensis* needs to be redescribed.

Compared to the original research article, this study re-examines *Liaoningotitan sinensis* more comprehensively and uses the newest matrix of Titanosauriform dinosaurs to conduct the systematic phylogenetic analysis. First, individuals of the *Liaoningotitan sinensis* holotype were carefully reexamined and identified one new autapomorphic characteristic on the humerus. Second, the skull and body type of the *Liaoningotitan sinensis* holotype were reconstructed. The skull reconstruction refers to some sauropods whose skull is preserved well, such as *Euhelopus zdanskyi* and *Rapetosaurus krausei*. The reconstruction of body type refers to *Euhelopus zdanskyi*, using the method of dividing the length of the posterior vertebra by the length of the anterior vertebra one by one and then inputting the value into the vertebrae of *Liaoningotitan* (Lü et al., 2014). Finally, the phylogenetic position of *Liaoningotitan sinensis* was analyzed using the software TNT 1.5, the matrix used in the analysis from Beeston et al. (2024), the newest matrix of Titanosauriformes phylogenetic analysis.

Systematic paleontology

Saurischia Seeley, 1887

Sauropodomorpha Huene, 1932

Sauropoda Marsh, 1878

Titanosauriformes Salgado, Coria & Calvo, 1997

Somphospondyli Wilson & Sereno, 1998

Liaoningotitan sinensis Zhou et al., 2018

MATERIALS

The skull, partial cervical, dorsal, sacral, and caudal vertebrae, appendicular elements, and pelvic girdle of a single individual PMOL-AD00112 were preserved. However, the medial and posterior sides of all vertebrae and most appendicular elements of the *Liaoningotitan sinensis* holotype are covered by gypsum. Therefore, the observation and research on this individual specimen is limited.

Diagnosis. Premaxilla and maxilla are similar to that in early-diverging Titanosauriformes, quadratojugal is similar to that in late-diverging Titanosauriformes. The anterior side of the jugal is aligned with the anterior side of the antorbital fenestra (autapomorphy). The angle between the horizontal and ascending branches of the quadratojugal is obtuse (autapomorphy). The lacrimal presents a fossa. The neural spine of the posterior dorsal vertebra is not bifurcated. A shallow fossa is located in the posterior part of the neural spine of the dorsal vertebra (a new autapomorphy). The lateral pneumatic foramen of the dorsal vertebra is shallow. The middle caudal vertebra is procoelous (autapomorphy). The attachment point of the muscle coracobrachialis on the anterior surface of the proximal end of the humerus is flat (a new autapomorphy). The second cnemial crest of the tibia is absent. The preserved elements of the holotype are shown in [Fig. 2](#).

Description

Skull: Only the left side of the skull of the *Liaoningotitan sinensis* holotype is visible ([Fig. 3](#)) and is approximately 30 cm in length (the preserved most anterior part of the premaxilla to the preserved most posterior part of the quadratojugal) and 20 cm in height (the preserved apex of the narial to the preserved bottom of the quadratojugal), with no developed premaxillary fenestra. The antorbital fenestra is well-defined and triangular, similar to those in *Euhelopus zdanskyi* ([Poropat & Benjamin, 2013](#)), *Mamenchisaurus youngi* ([Ouyang, 2003](#)), and *Omeisaurus maoianus* ([Tang et al., 2001](#)). The orbit is broken. The narial fenestra opens laterally. It does not exhibit a conspicuous anteroposterior expansion, similar to those of the early-diverging Titanosauriformes such as *Euhelopus zdanskyi*, but differing from those of the late-diverging Titanosauriformes such as *Rapetosaurus krausei* ([Rogers & Forster, 2004](#)). The length of the premaxilla constitutes 15% of the skull's overall length (the preserved most anterior part of the premaxilla to the preserved most posterior part of the preserved quadratojugal). The premaxilla and maxilla are divided by a suture. The length of the maxilla is three times the length of the dentigerous portion of the maxilla. The anterior side of the jugal is aligned with the anterior side of the antorbital fenestra, representing an autapomorphy. The maxilla is connected with quadratojugal bone, and the posterior region of the maxilla arch towards the dorsal side, similar to that in the late-diverging Titanosauriformes such as *Rapetosaurus krausei* ([Rogers & Forster, 2004](#)). The right lacrimal is preserved and isolated. The form of the lacrimal is similar to those seen in *Euhelopus zdanskyi*. A fossa presents in the dorsal portion of the lacrimal, speculation that is connected to the maxilla, similar to that seen in *Euhelopus zdanskyi* and *Tapuiasaurus macedoi* ([Wilson & Upchurch, 2009](#); [Wilson et al., 2016](#)). However, the lacrimal shaft's dorsal portion is thinner than the ventral portion, dissimilar to that seen in

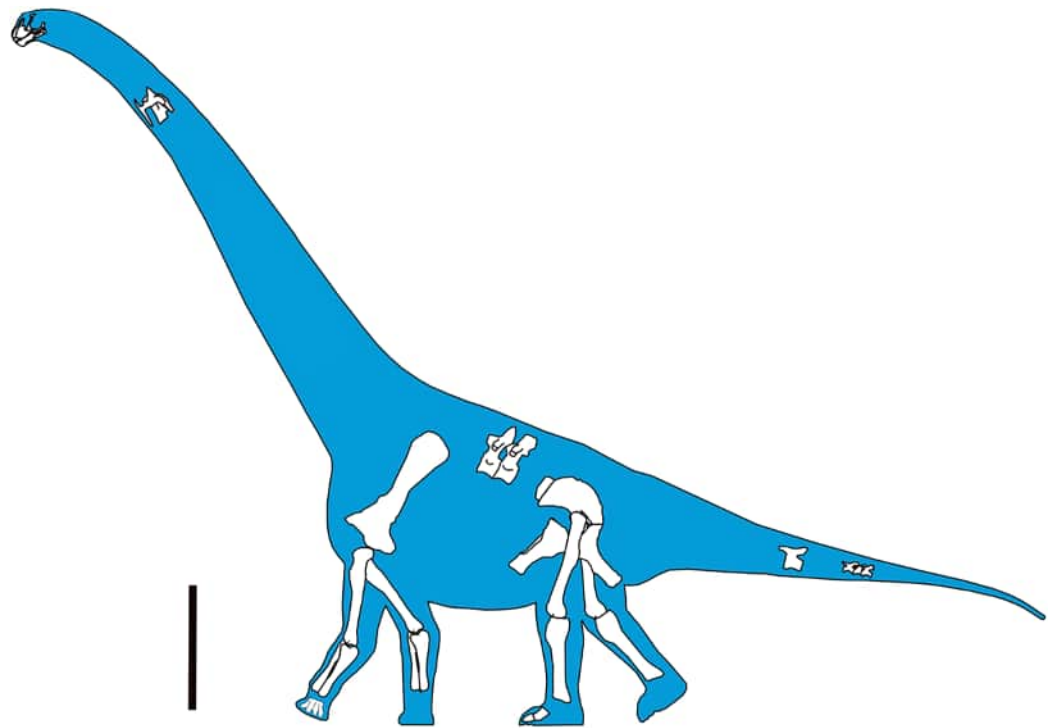


Figure 2 Preserved elements of *Liaoningotitan sinensis* holotype PMOL-AD00112. Edited from *Euhelopus zdanskyi*, a preserved complete Titanosauriform dinosaur. Painted by Gallipus (a net ID of helper <https://www.deviantart.com/ty2000>) Scale bar: 1 m.

Full-size  DOI: 10.7717/peerj.19154/fig-2

Euhelopus zdanskyi and other Somphospondyli whose lacrimal bones are thick, but similar to that seen in Brachiosauridae (Wilson & Upchurch, 2009; Wilson et al., 2016; Martinez et al., 2016; Poropat et al., 2023; Rogers & Forster, 2004; Wilson & Sereno, 1998; Daniel et al., 2010). The palatine is a laminar and triradiate bone with a maxillary branch. The pterygoid is also triradiate, with a fan-shaped anterior process. The angle between the horizontal branch and the ascending branch of the quadratojugal is an obtuse angle, similar to that found in some late-diverging Titanosauriformes such as *Rapetosaurus krausei* (Rogers & Forster, 2004) and *Tapuiasaurus macedoi* (Wilson et al., 2016). This differs from early-diverging Titanosauriformes such as *Euhelopus zdanskyi* and *Giraffatitan brancai*, indicating that mosaic evolution occurred in the skull of *Liaoningotitan sinensis*. The maxilla and quadratojugal cover the dorsal edge of the dentary, surangular, and angular. Because the surface of the mandibula is full of cracks, the borderline of these three bones is not obvious, as shown in the dotted line in Fig. 3B. The dentary is U-shaped and robust, with a circular rostral side. An obvious foramen is between the surangular and angular, the form is similar to the posterior surangular foramen of the non-Titanosauriformes Sauropod dinosaurs such as in the *Mamenchisauridae* (Ouyang, 2003; Yang, 2014), but has not been seen yet in the Titanosauriformes (Martinez et al., 2016; Poropat & Benjamin, 2013), therefore, our research is cautious about whether the foramen is the posterior surangular foramen or not. The teeth are spoon-shaped with narrow crowns and are only distributed in the anterior

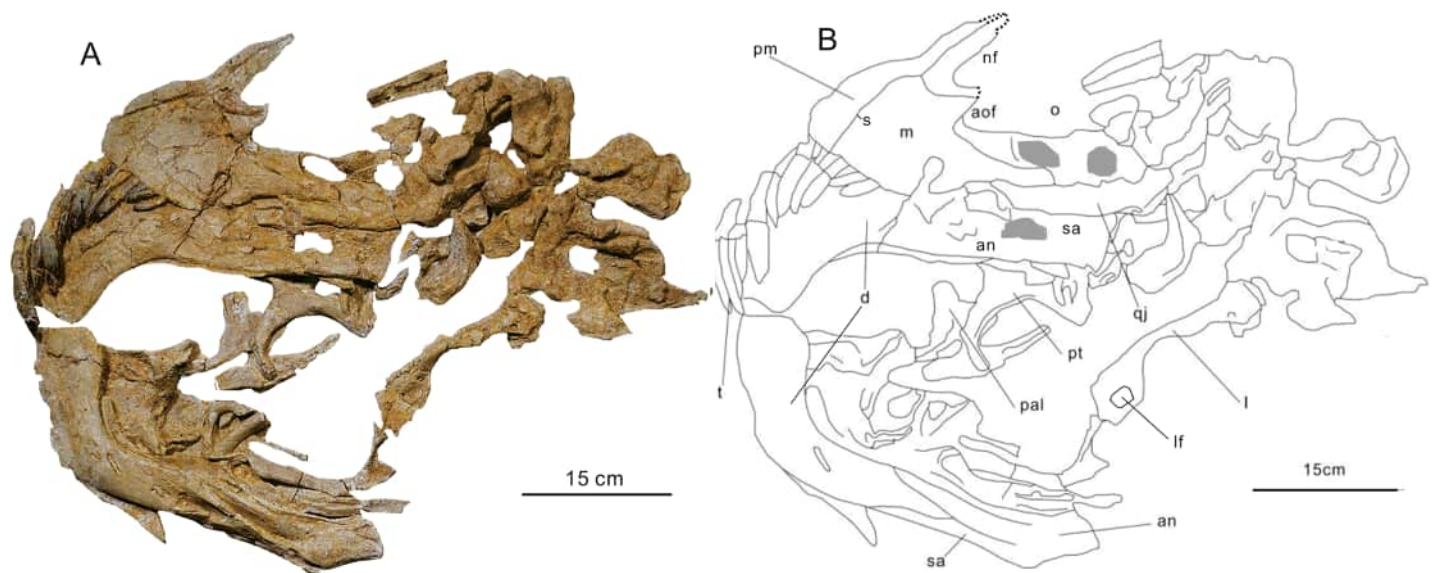


Figure 3 Skull of *Liaoningotitan sinensis* holotype PMOL-AD00112. Scale bar: 15 cm. (A) Photograph; (B) Line drawing. Dotted line in the line drawing: broken area. Gray area in the line drawing: foramen. Abbreviations: an, angular; aof, antorbital fenestra; d, dentary; f, foramen; j, jugal; l, lacrimal; lf, lacrimal fossa; m, maxilla; nf, narial fenestra; o, orbit; pal, palatine; pm, premaxilla; pt, pterygoid; qj, quadratojugal; s, suture; sa, surangular; t, teeth.

Full-size DOI: 10.7717/peerj.19154/fig-3

region of the premaxilla, and maxilla. The rostral is convex laterally and lingual concave to medial. The slender index of the teeth (the ratio of the tooth crown length to tooth crown width) is nearly 3.76. The cross-section of the crown is elliptical. The teeth had no serrations. The angle between the long axis of the tooth crown and the abrasive surface is approximately 30° . The ratio of the tooth crown and tooth root length is approximately 1.1. The skull is shown in Fig. 3.

Cervical vertebrae: Only one cervical vertebra is well preserved and 30 cm long. However, the anterior and posterior surfaces, prezygapophysis, and postzygapophysis of the vertebra are invisible (Fig. 4). Only the left surface of the vertebra is visible. The neural spine is bifurcated, A shallow pleurocoel is divided by a lamina on the lateral surface of the cervical vertebra, similar to that in *Bellusaurus sui* (Mo, 2013). The posterior centrodiapophyseal lamina connects the diapophysis. The cervical rib is a double-head type and short. The cervical vertebra preserves the caput costae. The cervical rib develops a rib ridge (Fig. 4B).

Dorsal vertebrae: There are only two preserved dorsal vertebrae (Fig. 4A), referred to as 'a' and 'b' for distinguishing (a: left dorsal vertebra in Fig. 4A, shown in left side view; b: right dorsal vertebra in Fig. 4A, shown in posterior side view). Both dorsal vertebrae are flat, also presumed to have been flattened by the rock bed.

Dorsal vertebra 'a' is a middle dorsal vertebra in speculation. The left surface of the dorsal vertebra 'a' is 17 cm long. The angle between the diapophysis and posterior centrodiapophyseal lamina is acute. The posterior centrodiapophyseal lamina and posterior centroparapophyseal lamina are intersected but do not form a K shape, dissimilar to that seen in the middle dorsal vertebrae of *Euhelopus zdanskyi* and *Gannansaurus*

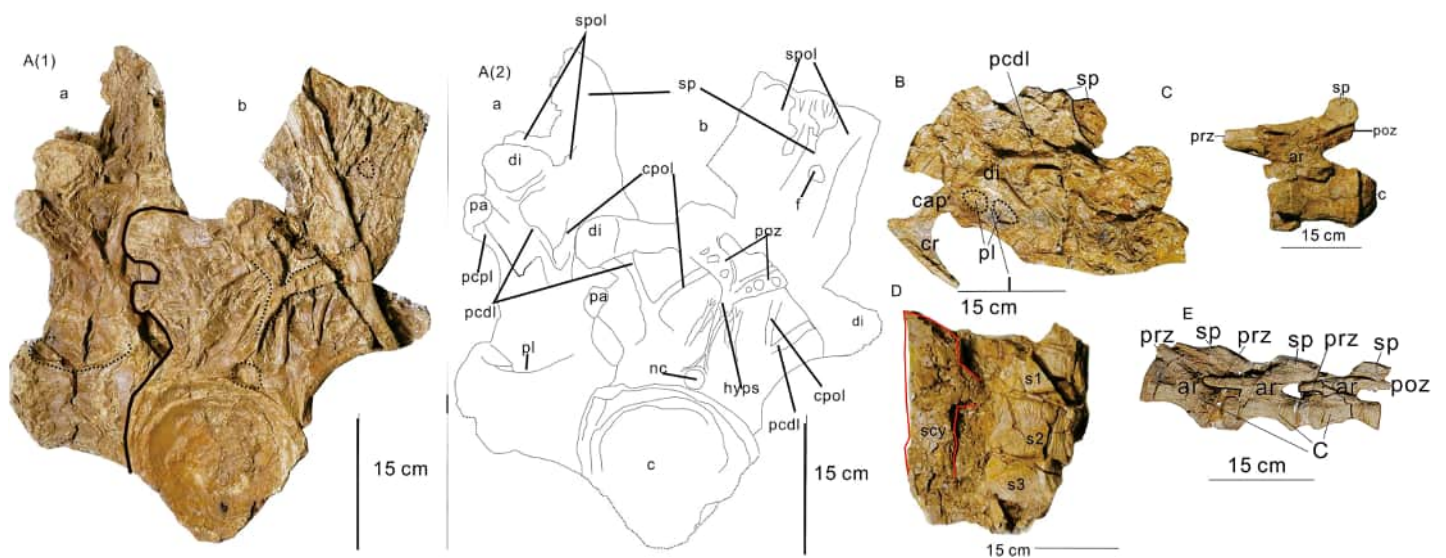


Figure 4 Vertebrae of *Liaoningotitan sinensis* holotype PMOL-AD00112. A(1) The photograph of the posterior dorsal vertebrae in left (a) and posterior (b) view. A(2) Posterior dorsal vertebrae a and b in line drawing. (B) Cervical vertebrae in left view. (C) Middle caudal vertebrae in left view. (D) Sacrum in right view. (E) Posterior caudal vertebra in left view. Dotted line: poz and hyps, pl, nc, f (A1); broken region (A2). Scale bar: 15 cm. Sacral yoke is marked by a red line. Abbreviations: ar, arch; c, centrum; cap, caput costae; cpol, centropostzygapophyseal lamina; cr, cervical rib; di, diapophysis; dr, dorsal rib; f, fossa; hyps, hyposphene; l, lamina; nc, neural canal; pa, parapophysis; pcdl, posterior centrodiapophyseal lamina; pcpl, post centroparapophyseal lamina; pl, pleurocoel; poz, postzygapophysis; prz, prezygapophysis; r, ridge on the cervical rib; s, sacrum; scy, sacral yoke; sp, spine; spol, spinopostzygapophyseal lamina.

Full-size [DOI: 10.7717/peerj.19154/fig-4](https://doi.org/10.7717/peerj.19154/fig-4)

sinensis (Wilson & Upchurch, 2009; Lü et al., 2013b). The diapophysis extends dorsolaterally (Fig. 4A), similar to that in the middle dorsal vertebra of *Liubangosaurus hei*, *Daxiatitan binglingi*, *Yongjinglong datangi* and *Euhelopus zdanskyi* (Mo, Xu & Buffetaut, 2010; You et al., 2008; Li et al., 2014; Wilson & Upchurch, 2009), therefore the article speculates ‘a’ is a middle dorsal vertebra. The angular surface of the diapophysis and parapophysis is elliptical. The lateral surface’s pleurocoel (pneumatic foramen) is shallow, similar to that seen in *Euhelopodidae* (Mannion et al., 2013). The dorsal edge of the pleurocoel is broken.

Dorsal vertebra ‘b’ is a posterior dorsal vertebra in speculation. The posterior angular surface of the centrum of vertebra ‘b’ is opisthocoelous and wider than its height. The ratio of lateromedially width to dorsoventral height of the centrum is 1.2, which is greater than that seen in *Daxiatitan binglingi* (You et al., 2008) and less than that seen in *Mamenchisaurus youngi* (Ouyang, 2003). The length of the neural spine is shorter than the centrum. A dorsal rib covers the left part of the neural spine. Only the left parapophysis is preserved. The diapophysis is vertical to the hyposphene and extends in a transverse orientation (extends laterally), therefore the article speculates ‘b’ is a posterior dorsal vertebra, similar to that seen in *Euhelopus zdanskyi*, *Patagotitan mayorum*, *Yongjinglong datangi* and *Daxiatitan binglingi* (Wilson & Upchurch, 2009; Carballido et al., 2017; Li et al., 2014; You et al., 2008). The location of the parapophysis is lower than the hyposphene. The width of the neural canal is greater than its length. The postzygapophysis and hyposphene are Y-shaped. The posterior centrodiapophyseal lamina and centropostzygapophyseal lamina constitute a shallow fossa, similar to that seen in the

Ruyangosaurus giganteus and *Daxiatitan binglingi* (Lü et al., 2014; You et al., 2008). The neural spine is not bifurcated, similar to that seen in Titanosauria (Mannion et al., 2013). The spinopostzygapophyseal laminae are narrow, and their lateral extension is not conspicuous. A shallow fossa is located on the right posterior side of the neural spine, we speculate there are two shallow fossae located on the posterior side of the neural spine but a dorsal rib covers the left one. The ventral profile of the centrum is incomplete, and the ratio of the dorsoventral height of the neural spine to the posterior angular centrum is 0.98 (Fig. 4A).

Sacral vertebrae: Sacral vertebrae I, II, III (s1, s2, s3) are preserved but embedded in the rock. All centra are amphiplatyan. All vertebrae preserve no neural arch and spine (Fig. 4D). s2 is well preserved, while s1 and s3 are fragmented. The left sacral yoke is preserved, and the form is plate-like. The vertebrae are rectangular, with the anterior and posterior regions equal in height. There are no apparent concavities on the lateral surface of the vertebrae. All vertebrae are interrelated but have not fused, suggesting that this specimen was still immature at death.

Caudal vertebrae: All caudal vertebrae are embedded in the rock, so only the left lateral faces are visible. The middle and posterior caudal vertebrae are preserved and interrelated, but only one middle and three posterior caudal vertebrae are completely preserved. They are all procoelous (Figs. 4C and 4E). The left lateral surface is visible with no diapophyses or concavities. The ventral surface has visible concavities, with the concavity of the anterior caudal centrum being shallower than that of the posterior caudal centra. The neural arch is in the front region of the vertebra and extends in an upper posterior orientation. The angle between the arch and vertebra is approximately 25°. In all preserved caudal vertebrae, the prezygapophysis is long, extending to the anterior, beyond the vertebra. The distance the prezygapophysis extends beyond the anterior margin of the centrum in the middle posterior neural arches is 49% of the centrum length, similar to that seen in Somphospondyli. The postzygapophysis of the middle caudal vertebra approximately is aligned with the posterior part of the centrum (Fig. 4E). The angle between the spine and vertebra is approximately 60°. In the posterior caudal vertebrae, postzygapophysis extends to the dorsoposterior and beyond the neural spine. No chevron bones are preserved in all caudal vertebrae. All vertebrae are shown in Fig. 4.

Scapula: The left scapula is preserved. The proximal end extends dorsolaterally. The dorsal side is thick, and the ventral side is thin. The proximal end is medially curved, similar to that in Somphospondyli. The ratio of the maximum dorsoventral height to the minimum dorsoventral height of the scapular blade is 1.2, less than that of *Dashanpusaurus dongi* (Ren, 2020; Ren et al., 2022) and *Jiangshanosaurus lixianensis* (Mannion et al., 2019a). The scapula has a lateral ridge in the middle of the shaft and extends to the anterior and posterior, similar to that of *Jiangshanosaurus lixianensis* (Mannion et al., 2019a), and speculated to be the attachment point of the subcoracoscapularis muscle. The ratio of the overall length of the scapular blade to its narrowest dorsoventral length is 5.06. The acromion process is not preserved. The posterior margin of the acromial plate is concave. The angle between the acromion posterior region and the scapular shaft long axis is 37°. A subtriangular process in the

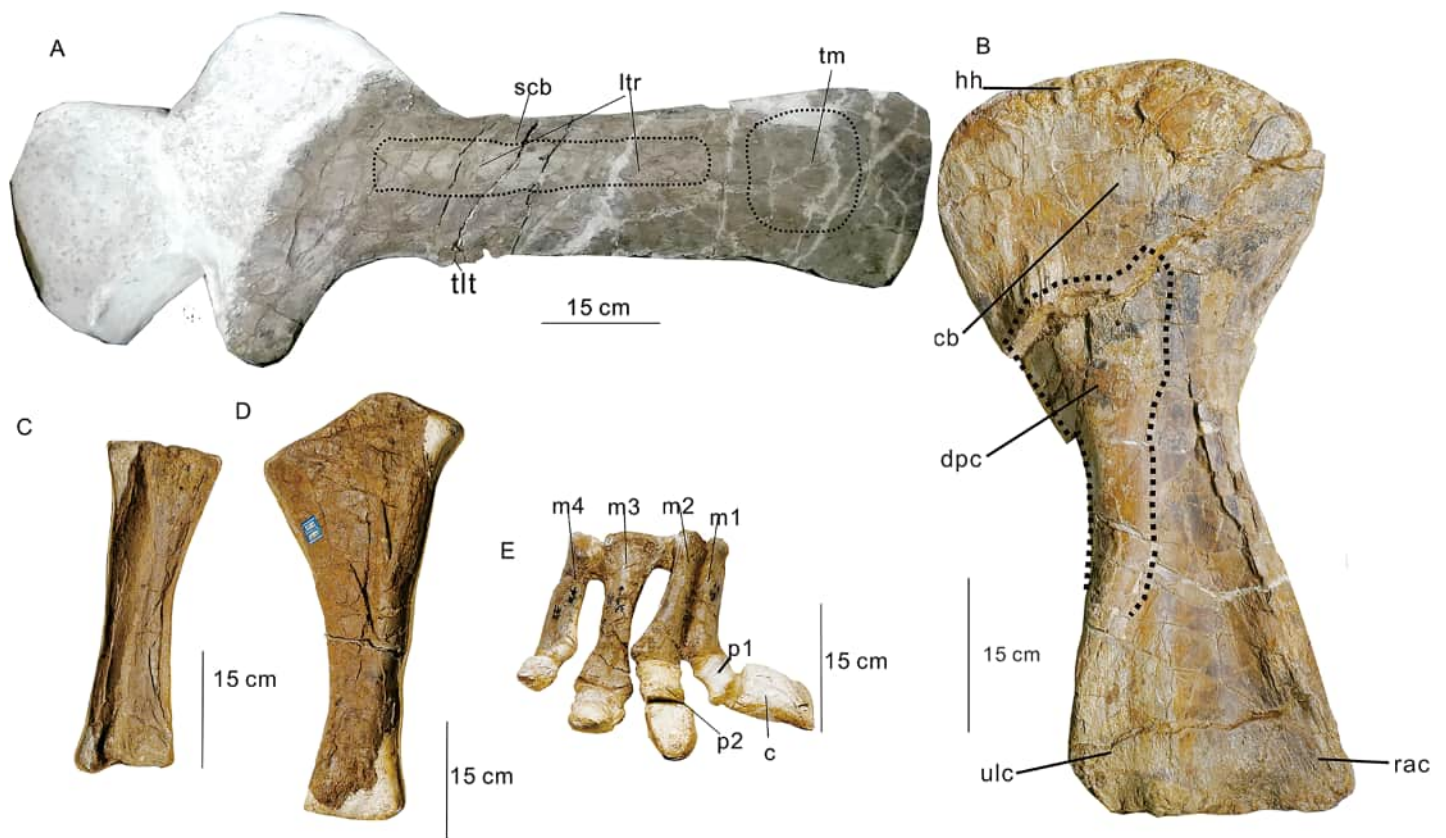


Figure 5 Left scapula (see in left lateral view) and forelimbs (see in anterior view) of the *Liaoningotitan sinensis* holotype PMOL-AD00112. (A) Scapula. (B) Humerus. (C) Radius. (D) Ulna. (E) Manus. Dotted line in the humerus: deltopectoral crest. Scale bar: 15 cm. Abbreviations: c, claw; cb, attachment point of coracobrachialis; dpc, deltopectoral crest; hh, humeral head; ltr, lateral ridge; m, metacarpus; p, phalanx; radial condyle; scb, scapular blade; tlt, attachment point of muscle triceps brachialis; tm, attachment point of muscle teres major; ulc, ulnar condyle.

Full-size [DOI: 10.7717/peerj.19154/fig-5](https://doi.org/10.7717/peerj.19154/fig-5)

anteroventral corner of the scapular blade is the tuberosity, or called the attachment point of the triceps brachii muscle, similar to that in *Yongjinglong datangi* and *Daxiatitan binglingi* (Li et al., 2014; You et al., 2008). The scapular suture and coracoid are lost. The cross-section of the middle region of the scapular shaft is D-shaped. The thickest area of the shaft is located in the 1/3 area of the proximal end. The width of the proximal end is 38% of the overall length of the scapula. The dorsoventral height of the distal end is greater than the dorsoventral height of the proximal end, and the dorsal side of the proximal end extends slightly to the dorsoventral and posterior side. The distal end extends to the dorsoposterior and posterior side, with an attachment point of the teres major muscle located on the lateral distal end of the scapula (Fig. 5A).

Humerus: Both the left and right humerus are well preserved. The humerus is short, with a length around 70% of the femur. The proximal end is fan-shaped; its maximum width is 54% of the length of the humeral shaft, and the minimum width of the proximal end is 31% of the length of the humeral shaft, which is greater than in Brachiosauridae. The proximal end extends lateromedially, indicating a robust forelimb. The lateral and medial surfaces of the humerus are asymmetric, and the medial angle is sharper than the lateral

angle. The slender index, or the humerus length ratio to the humerus's midshaft width, is 4.4, less than that of *Fusuisaurus zhaoi* (Mo et al., 2020). Proximal humeral robusticity (PHR), or the ratio of the length of the proximal end to the width of the midshaft, is 2.3, which is less than those of both *Ruyangosaurus giganteus* (Lü et al., 2014) and *Notocolossus gonzalezparejasi* (González Riga et al., 2016). The humeral head is oval-shaped. The muscle scar located in the anterior middle region of the proximal end is speculated to be the attachment point of the coracobrachialis muscle. This muscle scar is slightly flat rather than concave, dissimilar in the Mamenchisauridae, *Ruyangosaurus giganteus*, *Patagotitan mayorum* (Yang, 2014; Lü et al., 2014; Carballido et al., 2017), and other Titanosauriform dinosaurs, indicating that this is an autapomorphy of *Liaoningotitan sinensis*. The cross-section of the humeral shaft is elliptical. The humerus decreases in size from the proximal end to the distal end. The dorsal side of the deltopectoral crest is broken. The deltopectoral crest is robust, located in the 1/3 shaft region, and extends medially, similar to that in Titanosauria (Mannion et al., 2013). The length of the deltopectoral crest is 26% of the shaft's length, less than that seen in *Omeisaurus tianfuensis* and *Huangshanlong anhuiensis* (Ren, 2020). The deltopectoral crest is the attachment point of the pectoralis muscle. The concave shaft is not conspicuous and is located on the medial side of the deltopectoral crest. The width of the distal end is 41% of the shaft length of the humerus. The narrowest width of the middle of the shaft is 54% of the distal end's widest measurement. The radial and ulnar condyles are well preserved, extending to the distal end, with almost a 51° angle. The ulnar condyle is slightly larger than the radial condyle. The medial part of the ulnar condyle is greater than the lateral part (Fig. 5B). The robust index of the humerus, or the ratio of the average of the sum of the widest parts of the proximal end, middle, and distal end to the total length of the humeral shaft is 0.38, which is greater than the 0.29 robust index of the humerus in *Qingxiusaurus youjiangensis* (Mo et al., 2008), and less than the 0.39 robust index of the humerus in *Zhuchengtitan zangjiazhuangensis* (Mo et al., 2017), the humeral measurements of some Titanosauriformes shown in Table 2.

Radius: Only the left radius is preserved, 42 cm long, robust, and straight. The width of the proximal end is 25% of the total length. The cross-section of the middle of the shaft is elliptical (Fig. 5C).

Ulna: Only the left ulna is preserved, triradiate (Fig. 5D), and is 53 cm long. The width of the proximal end is 26 cm, and the width of the distal end is 12 cm.

Manus: Only the right manus is preserved. Metacarpus I–IV (m1–4) and two phalanges (p1 and p2) are preserved (Fig. 5E). The distal end of metacarpus I, II, and III extend, similar to a manus from an unnamed sauropod dinosaur excavated from the Tuchengzi Formation, Liaoning Province, China (Dong, 2001). The middle region of the metacarpus is thin. Phalanx III and IV are fused with the metacarpus. The length of the proximal end of metacarpus II is 27% of the overall length of metacarpus II. Metacarpus III is the longest. The length of all metatarsals is greater than their width. The medial surface of metacarpus IV is slightly concave. Phalanx I and phalanx II are covered by gypsum. Phalanx I has a robust claw (Fig. 5), speculated to have been used to defend against carnivorous theropods or attack competitors during courtship. The scapula and all forelimbs are shown in Fig. 5.

Table 2 Humerus measurements in some Titanosauriformes.

| Species | Proximal end length (mm) | Width midshaft (mm) | PHR | References |
|--|--------------------------|---------------------|------|---|
| <i>Liaoningotitan sinensis</i> | 400 | 170 | 2.35 | This article |
| <i>Notocolossus gonzalezparejasi</i> | 720 | 255 | 2.88 | González Riga et al. (2016) |
| <i>Patagotitan mayorum</i> | 560 | 270 | 2.07 | Otero, Carballido & Moreno (2020) |
| <i>Fusuisaurus zhaoi</i> | 565 | 215 | 3.07 | Mo et al. (2020) |
| <i>Ruangosaurus giganteus</i> (referred) | 540 | 320 | 1.68 | Lü et al. (2014) |
| <i>Rapetosaurus krausei</i> | 203 | 86 | 2.36 | Rogers (2009) |
| <i>Paralititan stromeri</i> | 562 | 234 | 2.40 | Smith et al. (2001) |
| <i>Futalognkosaurus dukei</i> | 600 | 250 | 2.40 | Calvo (2014) |
| <i>Dreadnoughtus schrani</i> | 740 | 320 | 2.31 | Lacovara et al. (2014) |
| <i>Qingxiusaurus youjiangensis</i> | 370 | 155 | 2.38 | Mo et al. (2008) |

Note:

PHR, proximal humeral robusticity.

Ilium: The ilium is approximately 70 cm long and not fused with the sacrum. The ilium is elliptical and slightly concave in lateral view, and the dorsal side bulges into an arch, similar to that in *Analong chuanjieensis* ([Ren, 2020](#)). The dorsoventral height of the ilium is 42% of the overall length of the ilium. The lateral side of the ventral surface bulges slightly. The preacetabular process extends to the anterior, and the anterior end is acute and triangular, which is different from that in *Qiaowanlong kangxii* ([Li & You, 2009](#)), *Dongyangosaurus sinensis* ([Lü et al., 2008](#)), and *Ruyangosaurus giganteus* ([Lü et al., 2014](#)), but similar to that in *Qinlingosaurus luonanensis* ([Xue et al., 1996](#)). The preacetabular angle is 50°, which is less than that in *Qinlingosaurus luonanensis* ([Xue et al., 1996](#)) and greater than that in *Dongyangosaurus sinensis* ([Lü et al., 2008](#)), but similar to the angle seen in *Shunosaurus lüi* ([Zhang, 1988](#)) and *Mamenchisaurus youngi* ([Ouyang, 2003](#)). The lateral side of the postacetabular process is flat ([Fig. 6](#)), unlike *Ruixinia zhangii*, which has a distinct bulge on the lateral side of the postacetabular process ([Mo et al., 2022](#)). The acetabulum is semicircular.

Pubis: The pubic bone is approximately 77 cm in length. The proximal end is plate-like and flat, and the shaft is not inflated. The acetabulum is semicircular. The pubic foramen is an elliptical shape ([Fig. 6](#)). The pubic apron is located on the ventral aspect of the pubis. The length of the articular surface of the ilium is 19% of the pubis shaft's length.

Ischium: The ischium is approximately 70 cm in length, Y-shaped, and triradiate, similar to that in *Huanghetitan ruyangensis* ([You et al., 2006](#)). The dorsoventral length of the proximal end is twice that of the distal end and is 57% of the overall length. The middle region of the proximal end is flat. The iliac process is triangular. The acetabulum is semicircular and conspicuously concave ([Fig. 6](#)). The ratio of the dorsoventral width of the ischium's distal shaft to the ischium's proximodistal length is 0.24. The ratio of the anteroposterior length of the proximal plate to its total length is 0.67. The ratio of the dorsoventral width of the distal end of the ischial shaft to the smallest dorsoventral width of the shaft is 0.9, similar to that in Somphospondylans ([Mannion et al., 2013](#)). The pelvic girdle is shown in [Fig. 6](#).

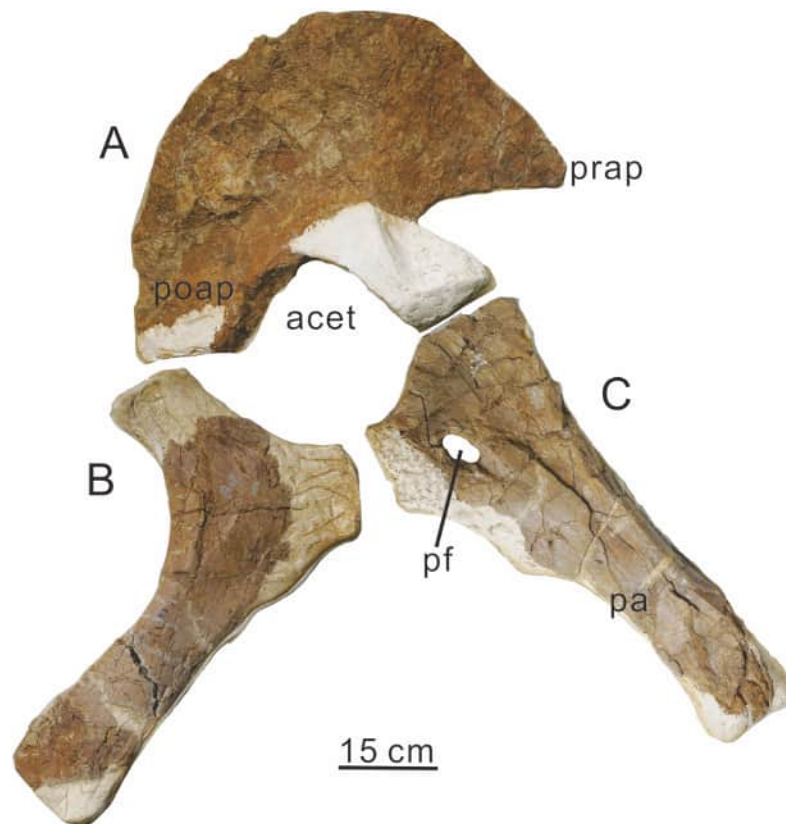


Figure 6 Right pelvic girdle (see in right lateral view) of *Liaoningotitan sinensis* holotype PMOL-AD00112. (A) Ilium. (B) Ischium. (C) Pubis. Scale bar: 15 cm. Abbreviations: acet, acetabulum; pa, public apron; pf, pubic foramen; poap, postacetabular process; prap, preacetabular process.

Full-size  DOI: [10.7717/peerj.19154/fig-6](https://doi.org/10.7717/peerj.19154/fig-6)

Femur: The right femur is 106 cm long and only the anterior side is visible. The width of the proximal end is 36 cm and the width of the distal end is 40 cm. The width of the proximal end is 34% of the total length of the femur. A distinct lateral bulge is located at the proximal end's lateral margin, similar to that in *Yunmenglong ruyangensis* and *Patagotitan mayorum* (Lü *et al.*, 2013a; Carballido *et al.*, 2017). The femoral head is well developed and is confluent with the proximal end, lacking a distinct neck. The angle between the dorsal margin of the proximal end and the lateral margin is 127°. The shaft is long and robust with an elliptical cross-section (Fig. 7). The greater trochanter is not conspicuously developed. The lateral process is located in the lower part of the greater trochanter and is 1/3 of the shaft's lateral dimension. In the distal end, the fibular and tibial condyles extend laterally and are concave. The Femoral Robusticity Index (FRI), or the ratio of the sum of the widths of the proximal, middle, and distal ends to the total femur length, is 0.94, greater than that of *Ruyangosaurus giganteus* and *Daxiatitan binglingi* (Lü *et al.*, 2014; You *et al.*, 2008). The medial margin of the femur is concave, similar to that in *Ruyangosaurus giganteus* (Lü *et al.*, 2014). The femoral measurements of some Titanosauriformes are shown in Table 3.

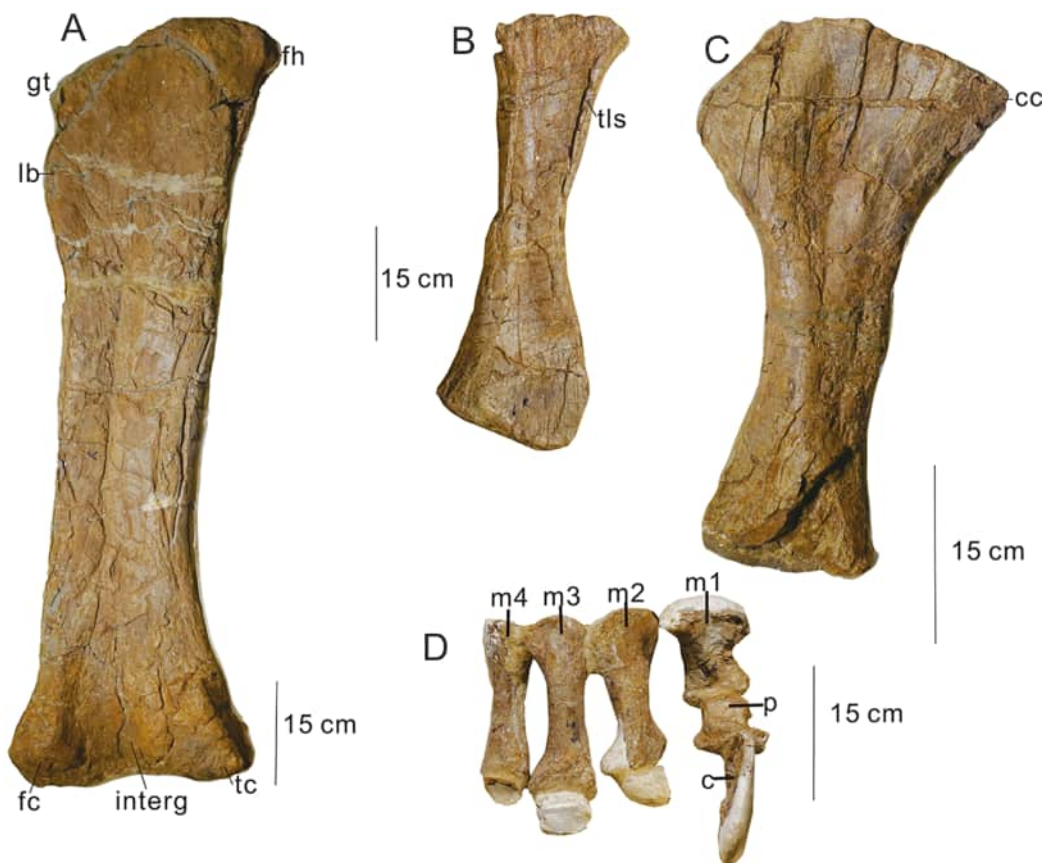


Figure 7 Hindlimbs (see in anterior view) of *Liaoningotitan sinensis* holotype PMOL-AD00112. (A) Femur. (B) Fibula. (C) Tibia. (D) Pes. Scale bar: 15 cm. Abbreviations: c, claw; cc, cnemial crest; fc, fibular condyle; fh, femoral head; gt, greater trochanter; lb, lateral bulge; m, metatarsal; p, phalanx; tc, tibial condyle; tls, tibial ligament muscle scar.

Full-size [DOI: 10.7717/peerj.19154/fig-7](https://doi.org/10.7717/peerj.19154/fig-7)

Table 3 Femur measurements of some Titanosauriformes.

| Species | Midshaft minimum length (mm) | Femur total length (mm) | FRI | References |
|---|------------------------------|-------------------------|------|---|
| <i>Liaoningotitan sinensis</i> | 230 | 1,060 | 0.94 | This article |
| <i>Dongbeititan dongi</i> | 230 | 1,100 | 0.93 | Wang et al. (2007) |
| <i>Daxiatitan binglingi</i> | 300 | 1,770 | 0.81 | You et al. (2008) |
| <i>Ruyangosaurus giganteus</i> (referred) | 300 | 1,670 | 0.82 | Lü et al. (2014) |
| <i>Patagotitan mayorum</i> | 360 | 2,360 | 0.71 | Otero, Carballido & Moreno (2020) |
| <i>Yunmenglong ruyangensis</i> | 360 | 1,920 | 0.86 | Lü et al. (2013a) |
| <i>Opisthocoelicaudia skarzynskii</i> | 250 | 1,395 | 0.82 | Borsuk-Bialynicka (1977) |
| <i>Fushanosaurus qitaiensis</i> | 270 | 1,800 | 0.73 | Wang et al. (2019) |
| <i>Huabeisaurus allocotus</i> | 245 | 1,560 | 0.73 | D'Emic et al. (2013) |
| <i>Rapetosaurus krausei</i> | 177 | 657 | 0.70 | Rogers (2009) |

Note:

FRI, femoral robusticity index.

Tibia: The tibial length is 56% of the femoral length. The proximal end extends lateromedially. The tibial ridge is well-developed and extends laterally to the 2/3 position of the shaft. The ridge length is 94% of the width of the tibial proximal end. The fibular articular surface is concave and located behind the ridge. The 1/3 position of the tibia shaft extends. The narrowest position of the tibia is located below the middle point of the shaft and is 1/3 of the width of the proximal end. The distal end extends to both the anterior and posterior. Cnemial crest develops well. The second cnemial crest is absent, similar to that in Euhelopodidae (Mannion *et al.*, 2013). The narrowest region of the tibial shaft is located above the center point of the tibial shaft (Fig. 7).

Fibula: The length of the fibula is slightly shorter than the length of the tibia and is half the length of the femur. The length of the proximal end of the fibula is 66% of the length of the proximal end of the tibia. The shaft of the fibula is straight and narrow with both mediolateral shrinkage evident. There is a tibial ligament muscle scar. The distal end of the fibula extends to lateromedially and is convex medially (Fig. 7).

Pes: The right pes is preserved. Metatarsal I–IV (m1–4) and one phalanx (p) are preserved (Fig. 7). The pes has a developed, robust, and flat claw. The lateral and medial sides of all metatarsals are curved. The claws are regressed in metatarsals II to IV, and the phalanges are fused with the metatarsals. Metatarsal I is robust and short, with a proximal end that extends slightly. The length of metatarsal I is 30% of radial length and 63% of the length of metatarsal II. The phalanx is robust. Metatarsal II is 20 cm long and is distinctly longer and narrower than metatarsal I, similar to those in *Opisthocoelicaudia* and *Notocolossus* (Borsuk-Bialynicka, 1977; González Riga *et al.*, 2016). The width of the proximal end of metatarsal II is narrower than the distal end. The ratio of the length of metatarsal II to its radial length is 0.2. Metatarsal III is the longest, but the ratio of the length of its proximal end to its radial length is also 0.2. The lateral profile of metatarsal III is convex. The shaft of metatarsal IV is the thinnest one of the metacarpus. The width of its proximal end is equal to the width of its distal end (Fig. 7). The ratio of the length of metatarsal IV to the radial length is 0.1. The hindlimbs are shown in Fig. 7.

Skull reconstruction

The skull of the *Liaoningotitan sinensis* holotype has preserved premaxilla, maxilla, dentary, angular, and supraangular bones, partial quadratojugal bones, and some teeth. An apparent slope between the premaxilla and maxilla is present, and the naris opens laterally. These characteristics are similar to those in *Mamenchisaurus youngi* (Ouyang, 2003), *Omeisaurus maoianus* (Tang *et al.*, 2001), and early-diverging Titanosauriformes such as *Euhelopus zdanskyi* (Poropat & Benjamin, 2013). Therefore, in our research, the nasal, maxilla, parietal, and frontal bones of *Euhelopus zdanskyi* were used as references for reconstructing the same parts of *Liaoningotitan sinensis*. However, the quadratojugal of *Liaoningotitan sinensis* differs from that in *Mamenchisaurus youngi*, *Omeisaurus maoianus*, and *Euhelopus zdanskyi*. The angle between the horizontal and the ascending branches of the quadratojugal of *Mamenchisaurus youngi*, *Omeisaurus maoianus*, and *Euhelopus zdanskyi* is close to a right angle, but in *Liaoningotitan sinensis*, the angle between the horizontal branch and ascending branch of the quadratojugal is obtuse. This

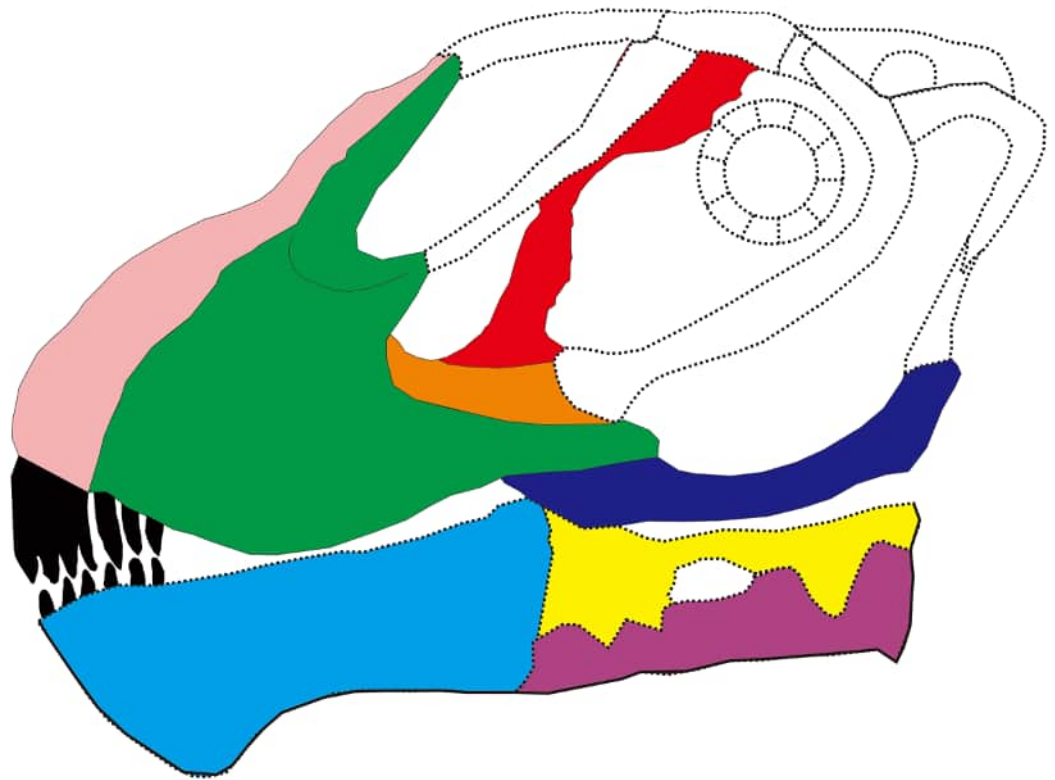


Figure 8 Reconstruction of the skull of *Liaoningotitan sinensis* holotype PMOL-AD00112. All unsaved and uncertain parts are shown in dotted lines. [Full-size !\[\]\(5f471a71b78d7676bc356df190b88ab4_img.jpg\) DOI: 10.7717/peerj.19154/fig-8](https://doi.org/10.7717/peerj.19154/fig-8)

characteristic is more similar to that of the late-diverging Titanosauriformes, such as *Nemegtosaurus mongoliensis* (Wilson, 2005), *Tapuiasaurus macedoi* (Wilson et al., 2016), and *Rapetosaurus krausei* (Rogers & Forster, 2004), indicating that the skull of *Liaoningotitan sinensis* is in a transitional state in the evolution from the early-diverging Titanosauriformes to the late-diverging Titanosauriformes. Therefore, it is speculated that the postorbital bones of *Liaoningotitan sinensis* are similar to those of the late-diverging Titanosauriformes. Our research used the postorbital, squamosal and quadrate of *Rapetosaurus krausei* to reconstruct the same parts of the *Liaoningotitan sinensis*. The result of the *Liaoningotitan sinensis* skull reconstruction is shown in Fig. 8.

Body type estimation

The *Euhelopus zdanskyi* was used for estimating the body length of the *Liaoningotitan sinensis* because the *Euhelopus zdanskyi* is a well-preserved sauropod dinosaur specimen with a complete skull, appendicular elements, cervical, and dorsal vertebrae. It was unearthed from the Lower Cretaceous Mengyin Formation in Ningjiagou village, Xintai City of Shandong Province, China, and housed in the Uppsala University of Sweden at the moment (Wilson & Upchurch, 2009). It was recovered as a member of the Somphospondyli family (Mannion et al., 2013, 2019a). The ratio of the length of the posterior vertebra to the length of the anterior vertebra (such as dorsal vertebra 2/dorsal vertebra 1) of the *Euhelopus zdanskyi* was calculated and then applied to the vertebrae of *Liaoningotitan*

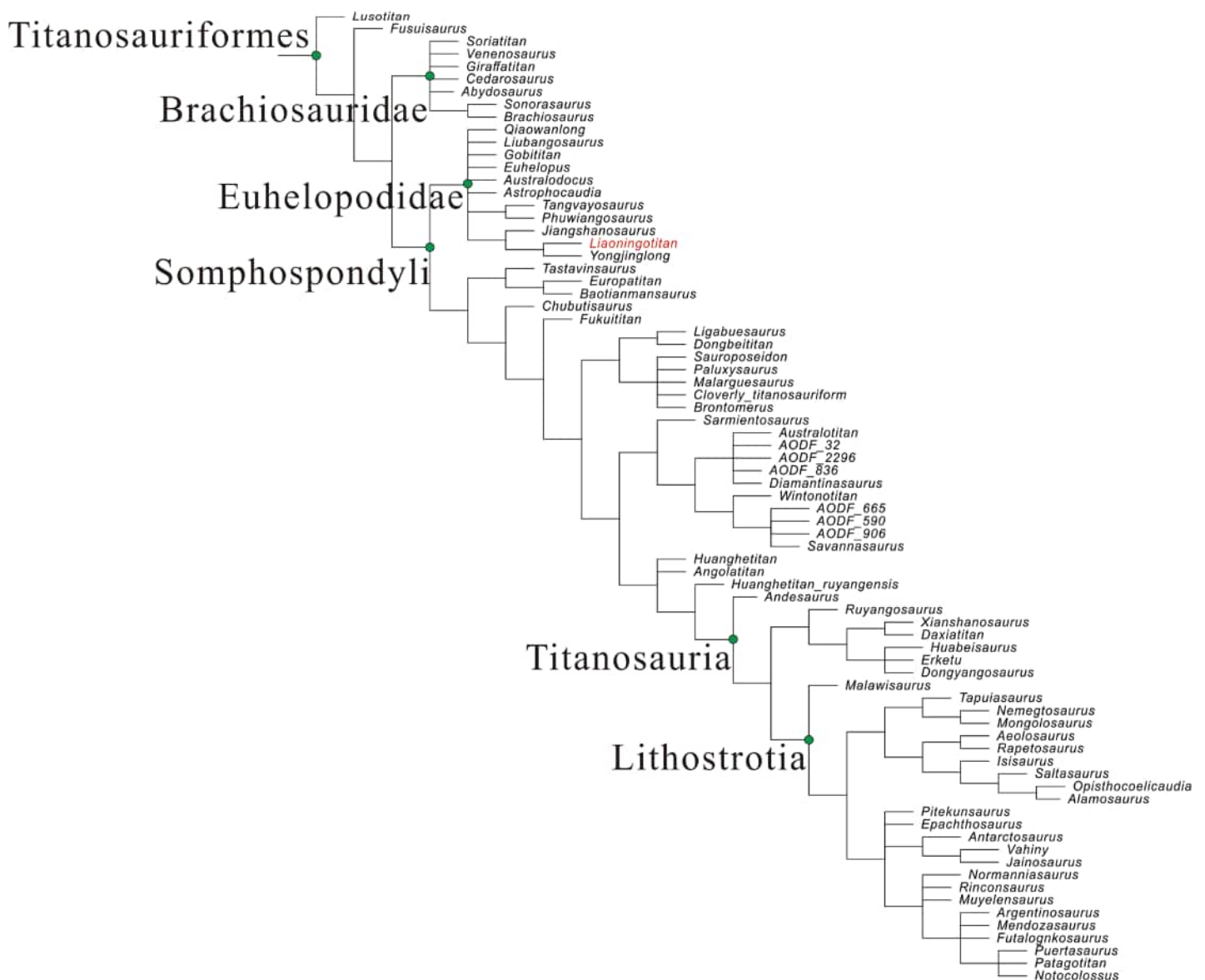


Figure 9 Phylogenetic analysis of strict consensus tree of *Liaoningotitan sinensis* (red). Matrix from *Beeston et al. (2024)*.

Full-size DOI: 10.7717/peerj.19154/fig-9

sinensis. The method was once used to reconstruct the body type of *Ruyangosaurus giganteus* (Lü *et al.*, 2014). The result indicated that the total length of the *Liaoningotitan sinensis* holotype is approximately 10 m. The height of the scapula and the lengths of the humerus, ulna, metacarpus, and pes all indicated that the *Liaoningotitan sinensis* specimen had a body length of approximately 10 m and a shoulder height of approximately 2 m. However, the sacral vertebrae of the *Liaoningotitan sinensis* holotype are not fused, indicating the holotype is an immature specimen. Hence, the body of a mature *Liaoningotitan sinensis* was probably larger.

Phylogenetic analysis

The first phylogenetic analysis of *Liaoningotitan sinensis* was performed in 2018, using a matrix modified from [Wilson & Upchurch \(2009\)](#). The results showed that *Liaoningotitan sinensis* was a Somphospondyliian clade member ([Zhou et al., 2018](#)). To further analyze the phylogenetic location of *Liaoningotitan sinensis*, this study used the matrix modified from [Beeston et al. \(2024\)](#) in TNT 1.5 software ([Goloboff & Catalano, 2016](#)) for the phylogenetic analysis, which the matrix includes 131 taxa (OTUs: Operational Taxonomic Units) and 560 characteristics. *Liaoningotitan* was added as a genus to the matrix. This study added the *Liaoningotitan* taxon to the matrix. Extended implied weighting (EIW) analyses were used with the following settings: max.trees was set to 10,000; tree bisection and reconnection (TBR) was used; new technology search was selected; random addition sequences were changed from 1 to 1,000 addseqs; sect search, ratchet, drift, and tree fusing were all used; The larger the weight set (the value of K), the smaller the weight of the isomorphic features, therefore our analysis attempted to set $K = 9$, similar in the previous analysis ([Mannion et al., 2019a](#); [Beeston et al., 2024](#)). All other options were set to default. The results showed that there were three strict consensus trees, a tree length of 2,840, a CI of 0.208, and a RI of 0.584. Standard bootstrap with the number of replicates changed from 100 to 5,000. Therefore, a strict consensus tree analysis was then performed. The final result identified *Liaoningotitan* within Euhelopodidae and constituted a sister group with *Yongjinglong*, as shown in [Fig. 9](#) (see matrix in [Supplemental Information](#)).

DISCUSSION

Four visible characteristics support the classification of *Liaoningotitan sinensis* within Somphospondyli: (1) the scapular glenoid surface is deflected, facing both anteroventrally and medially (Character 213); (2) the tibia lacks a 'second cnemial crest' (C261); (3) the ratio of the dorsoventral width across the ischial distal shaft to the proximodistal length of the ischium is 0.2 or greater (C63); (4) Distance that prezapophyses extend beyond the anterior margin of the centrum in the middle-posterior caudal neural arches is 20% or more of the centrum length (excluding the condyle) (C193) ([Mannion et al., 2013](#)).

Three visible characteristics support the classification of *Liaoningotitan sinensis* within Euhelopodidae: (1) the dorsoventral height of the posterior dorsal neural spines divided by the posterior centrum dorsoventral height is less than 1.0 (C23); (2) the pneumatic foramen (pleurocoel) in the lateral surface of the dorsal centra is shallow (C144); (3) the presence of the subtriangular process in the anteroventral corner of the scapular blade (C216) ([Mannion et al., 2013](#)).

Four important synapomorphies support *Liaoningotitan sinensis* and *Yongjinglong datangi* as sister groups: (1) attachment point of muscle triceps longus tubercle located in the ventral side of the scapula; (2) attachment of muscle teres major located in the distal side of the scapula; (3) The diapophysis of the middle dorsal vertebra extends dorsally; (4) The diapophysis of the posterior dorsal vertebra extends lateromedially ([Li et al., 2014](#)).

Comparison between *Liaoningotitan* and other partial Somphospondylan in China from the Cretaceous Period:

Comparison between *Liaoningotitan* and *Dongbeititan*: Similarities between *Dongbeititan* and *Liaoningotitan* include a distinct bulge site at the lateral margin of the femur; the femoral head is confluent with the proximal end and has no developed neck; metatarsal I is shorter than metatarsal II–IV; and metatarsal II is narrower than metatarsal I. *Dongbeititan* differs from *Liaoningotitan* in the following ways: *Dongbeititan* has a broad pubis, with the distal end notably extending from the dorsoventral surface.

Comparison between *Liaoningotitan* and *Ruyangosaurus*: There are many differences between *Liaoningotitan* and *Ruyangosaurus*. The narrowest dorsoventral height of the *Ruyangosaurus* scapular blade is less than that of the *Liaoningotitan*. The RI of the humerus of *Ruyangosaurus* is less than that of *Liaoningotitan*. In *Ruyangosaurus*, two of the distal condyles of the femur are the same size, but in *Liaoningotitan*, the fibular condyle is bigger than the tibial condyle at the distal end of the femur. The anterior region of the *Ruyangosaurus* ilium is circular, rather than the sharp anterior region in the *Liaoningotitan*'s ilium. The dorsoventral height of the ilium divided by the overall length of the ilium of *Ruyangosaurus* is greater than in *Liaoningotitan*. The FRI of the *Ruyangosaurus* femur is less than that of the *Liaoningotitan* femur. The narrowest region of the tibial shaft of the *Ruyangosaurus* is behind the middle point of the tibial shaft, contrary to that in *Liaoningotitan*. The location of the cnemial crest of *Ruyangosaurus* is lower than in *Liaoningotitan*. The neural spine of the posterior dorsal vertebra of *Ruyangosaurus* is bifurcated. The pleurocoel of the dorsal vertebra of *Ruyangosaurus* is deeper than that of *Liaoningotitan*. *Ruyangosaurus* and *Liaoningotitan* have the following similarities: the suture between the scapula and coracoid is a straight line; the humeral deltopectoral crest extends to the medial surface; the proximal end of the scapula is curved inward; the ventral surface of the posterior dorsal vertebra is concaved (Lü *et al.*, 2014).

Comparison between *Liaoningotitan* and *Jiangshanosaurus*: These two taxa differ in many characteristics, such as the location of the diapophysis, which is lower than the hyposphere in *Jiangshanosaurus* but aligned with the hyposphere in *Liaoningotitan*. The angle between the arch and the centrum and the angle between the neural spine and the centrum of the middle-posterior caudal vertebra of *Jiangshanosaurus* are greater than those in *Liaoningotitan*. The pleurocoel of the dorsal vertebra of *Jiangshanosaurus* is noticeably deeper than in *Liaoningotitan*. *Jiangshanosaurus* and *Liaoningotitan* share the following similarities: the dorsal vertebrae are opisthocoelous, the pubis is flat, and the length of the neural arch is longer than the posterior caudal vertebra (Mannion *et al.*, 2019a).

Comparison between *Liaoningotitan* and *Dongyangosaurus*: There are many differences between *Dongyangosaurus* and *Liaoningotitan*. All the neural spines of the dorsal vertebrae of *Dongyangosaurus* are short and bifurcated, and the pleurocoel of the posterior dorsal vertebrae of *Dongyangosaurus* is deeper than that of the dorsal vertebrae of *Liaoningotitan*. The diapophysis of the posterior dorsal vertebrae in *Dongyangosaurus* is located at the caudodorsal of the parapophysis. The lateral view of the ilium of *Dongyangosaurus* is convex, contrary to that of *Liaoningotitan*. The anterior process of the ilium of

Dongyangosaurus is blunt, and the anterior process of the ilium of *Liaoningotitan* is subtriangular. The pubis of *Dongyangosaurus* is shorter than its ischium, but the pubis and ischium are approximately equal in *Liaoningotitan*. *Dongyangosaurus* and *Liaoningotitan* share some similarities, such as the slightly concave ventral side of the dorsal vertebrae and the short diapophyses with circular surfaces extending laterally. The facets of the diapophysis are larger than the parapophysis in both *Dongyangosaurus* and *Liaoningotitan*, and the shaft of the ischium in both dinosaurs is plate-like (Lü *et al.*, 2008).

Comparison between *Liaoningotitan* and *Yongjinglong*: In the present analysis, *Liaoningotitan* constituted a sister group to *Yongjinglong*. There are many similar characteristics in *Liaoningotitan* and *Yongjinglong*, such as a medially-curved proximal end of the scapula and a D-shaped cross-section of the scapula. In both *Liaoningotitan* and *Yongjinglong*, the tuberosity of the triceps brachii muscles is located in the ventral side of the anterior side of the proximal end of the scapula (tlt), and the attachment point of the teres major muscle is located in the distal end of the scapula blade (tm). However, there are also many differences between *Liaoningotitan* and *Yongjinglong*: in *Yongjinglong*, the ventral side of the distal end of the scapula extends to the posterior, contrary to that in *Liaoningotitan*, and the dorsal and ventral sides of the scapular blade of *Yongjinglong* are approximately parallel (Li *et al.*, 2014).

Comparison between *Liaoningotitan* and *Euhelopus*: *Liaoningotitan* and *Euhelopus* have many similar characteristics, such as the narial fenestra in the skull opening laterally and the slope present in the anterior surface of the maxilla. In both *Liaoningotitan* and *Euhelopus*, the maxilla is part of the antorbital fossa, and the dorsoventral height of the posterior dorsal neural spines divided by the posterior centrum dorsoventral height is less than 1.0. The subtriangular process at the anteroventral corner of the scapular blade is speculated to be the tuberosity of the triceps brachii muscles in both taxa, which is also similar to *Yongjinglong*. The following differences are present between *Liaoningotitan* and *Euhelopus*: the dentition of *Euhelopus* extends to the posterior of the mouth and aligned with the anterior side of the antorbital fenestra, while the dentition of *Liaoningotitan* is limited to the anterior of the mouth; the anterior centrodiapophyseal lamina in the posterior dorsal vertebra of *Euhelopus* is well-developed and forms a K shape with the posterior centrodiapophyseal lamina and posterior centroparapophyseal lamina, but in the posterior dorsal vertebra of *Liaoningotitan* is not conspicuous (Poropat & Benjamin, 2013; Wilson & Upchurch, 2009).

Comparison between *Liaoningotitan* and *Huabeisaurus*: There are many similarities between *Liaoningotitan* and *Huabeisaurus*, such as an opisthocelous dorsal vertebra with a convex ventral side. *Liaoningotitan* and *Huabeisaurus* have a pleurocoel on the dorsal vertebra's lateral side. The neural arch of the caudal vertebra is situated in the anterior region. The neural spine of the dorsal vertebra is not bifurcated in either dinosaur, and both have a scapular shaft that is medially curved. *Liaoningotitan* and *Huabeisaurus* have a distinct lateral bulge on the femur. There are also many differences between *Liaoningotitan* and *Huabeisaurus*: the scapula of *Huabeisaurus* has no distinct subtriangular process; the preacetabular process of *Huabeisaurus* extends and is circular,

differing from the triangular preacetabular process of the ilium of *Liaoningotitan* (D'Emic *et al.*, 2013; Pang & Cheng, 2000).

Phylogenetic position of other Cretaceous Titanosauriformes in China

This analysis indicates that all genera of Cretaceous Titanosauriformes in China fit within Somphospondyli excluding *Fusuisaurus*. *Fusuisaurus* was reconsidered as a member of Basal-Titanosauriformes, supporting the result of the initial analysis (Mo *et al.*, 2006, 2020). *Liubangosaurus* was considered a non-Titanosauriformes Eusauropoda dinosaur in initial analysis (Mo, Xu & Buffetaut, 2010), then classified into Lithostrotia (Mannion *et al.*, 2013) or Euhelopodidae (Poropat *et al.*, 2014), and finally classified into Euhelopodidae again in the present analysis. *Yongjinglong*, *Qiaowanlong*, *Euhelopus*, and *Gobititan* have been classified into Euhelopodidae in many analyses (Mannion *et al.*, 2019b; Beeston *et al.*, 2024), and *Qiaowanlong* was considered a Brachiosaurid in an initial genus construction article (Li & You, 2009); the results of the present analysis support the classification of these genera into Euhelopodidae. *Dongbeititan* is classified as a non-Titanosauria Somphospondylan in the present analysis, which aligned with the results of previous analyses (Mannion *et al.*, 2019b; Poropat *et al.*, 2014), *Jiangshanosaurus* was classified as non-Euhelopodidae and Titanosauria Somphospondylan in the present analysis, but has been classified into Euhelopodidae and Lithostrotia in analyses of past time (Mannion *et al.*, 2013; Beeston *et al.*, 2024). In the present analysis, *Huanghetitan liujiaxiaensis*, *Huanghetitan ruyangensis*, and *Baotianmansaurus* are non-Euhelopodidae and Titanosauria Somphospondylan. *Huabeisaurus*, *Dongyangosaurus*, *Daxiatitan*, *Xianshanosaurus*, *Ruyangosaurus*, and *Mongolosaurus* are Titanosaurian. In past analyses, *Mongolosaurus* has been classified as Lithostrotian, and *Ruyangosaurus*, *Dongyangosaurus*, and *Jiangshanosaurus* have been identified as non-Titanosauria Somphospondylans (Poropat *et al.*, 2014; Mannion *et al.*, 2019a). The results of the present analysis support that *Xianshanosaurus* constitutes a sister group of *Daxiatitan*, and *Dongyangosaurus* constitutes a sister group of *Huabeisaurus*.

About Euhelopodidae

The present analysis supports the validity of Euhelopodidae. In this analysis, Euhelopodidae include *Euhelopus*, *Qiaowanlong*, *Erketu*, *Yongjinglong*, *Liubangosaurus*, *Tangvayosaurus*, *Gobititan*, *Phuwiangosaurus*, and *Liaoningotitan*. The result of the analysis supports that *Liaoningotitan* constituted a sister group with *Yongjinglong*, *Tangvayosaurus* constituted a sister group with *Phuwiangosaurus*. Fossil evidence has shown that the earliest taxon of Euhelopodidae in Asia is *Euhelopus*, from the Berriasian period in China (Han *et al.*, 2024). *Liaoningotitan*, *Yongjinglong*, *Euhelopus*, *Gobititan*, *Liaoningotitan*, *Qiaowanlong*, *Erketu*, *Tangvayosaurus*, *Phuwiangosaurus*, and *Liubangosaurus* indicate that Euhelopodidae was a large and diverse taxon in Asia during the Cretaceous Period. In addition, the present analysis identified *Australodocus* and *Astrophocaudia* as taxa of Euhelopodidae, indicating that the distribution region of Euhelopodidae might include Africa and North America. This conclusion will have to be verified in the future as fossil evidence continues to accumulate.

The Titanosauriformes skull

The current understanding of the evolution of the skull of Titanosauriformes is poor. As of February 2025, only 10 taxa of Titanosauriformes have been found with complete skulls: *Giraffatitan*, *Abydosaurus*, *Euhelopus*, *Liaoningotitan*, *Malawisaurus*, *Tapuiasaurus*, *Sarmientosaurus*, *Diamantinasaurus*, *Nemegtosaurus* and *Rapetosaurus*. Except for *Giraffatitan*, all of these taxa are from the Cretaceous Period, with *Abydosaurus*, *Euhelopus*, *Liaoningotitan*, *Malawisaurus*, and *Tapuiasaurus* coming from the Early Cretaceous. No individuals have been found from the Turonian-Campanian interval, making research on Titanosauriformes difficult (Paul, 1988; Wilson & Sereno, 1998; Daniel et al., 2010; Poropat & Benjamin, 2013; Zhou et al., 2018; Gomani, 2005; Wilson et al., 2016; Martinez et al., 2016; Beeston et al., 2024; Wilson, 2005; Rogers & Forster, 2004).

Based on the 10 taxa that have been found, Titanosauriformes skulls can be divided into four types by our research: (Type 1) In the first type, the snout is higher than the back of the skull (the nasal area bulges), all or most of the narial fenestra is visible in lateral view, and the angle between the horizontal and ascending branches of the quadratojugal is a right or acute angle, such as in *Giraffatitan*, *Abydosaurus*, *Euhelopus*, and *Malawisaurus*, and similar to the skulls of *Mamenchisaurus* and *Camarasaurus* (Daniel et al., 2010; Poropat & Benjamin, 2013; Zhou et al., 2018; Gomani, 2005; Ouyang, 2003). (Type 2) This type has a shorter snout compared to the back of the skull (nasal area is low), less of the narial fenestra is visible in lateral view, the skull is elongated in lateral view, and the angle between the horizontal and ascending branches of the quadratojugal is an obtuse angle, such as in *Tapuiasaurus*, *Nemegtosaurus* and *Rapetosaurus*, and similar to the skull of *Diplodocus* (Wilson et al., 2016; Wilson, 2005; Rogers & Forster, 2004). (Type 3) The skulls of *Sarmientosaurus* and *Diamantinasaurus* have a combination of characteristics of Titanosauriforme types 1 and 2. These have an elongated skull, with a nasal area taller than the back of the skull, a low narial fenestra, and an acute angle between the horizontal and ascending branches of the quadratojugal. These characteristics indicated that mosaic evolution occurred in the skull of *Sarmientosaurus* and *Diamantinasaurus*, and they are transitional species in the evolution of Titanosauriformes. (Type 4) *Liaoningotitan* has a bulging nasal area and an obtuse angle between the horizontal and ascending branches of the quadratojugal. Therefore, mosaic evolution also occurred in the skull of *Liaoningotitan*, and it is also a transitional species but contrary to those in *Sarmientosaurus* and *Diamantinasaurus* (Martinez et al., 2016; Poropat et al., 2023; Zhou et al., 2018). With more and more skulls of Titanosauriformes recorded and described in the future, types may increase, but at least one viewpoint will not be changed, is the mosaic evolution may be a common phenomenon in the skulls of Titanosauriformes and presents not only one evolutionary orientation, the evolution of Titanosauriformes may be more complex than we previously considered.

CONCLUSION

The *Liaoningotitan sinensis* holotype is a partial skeleton from the Lower Cretaceous Yixian Formation, a formation famous for Jehol Biota. It displays some characteristics that suggest *Liaoningotitan sinensis* is a valid species that can be distinguished from other

Titanosauriformes dinosaurs. This analysis classifies *Liaoningotitan sinensis* into Euhelopodidae, indicating that members of Euhelopodidae family inhabited this biota, which increases the known diversity of sauropod dinosaurs in the Jehol Biota. The research on the skull of *Liaoningotitan sinensis* holotype indicated that mosaic evolution is present in the *Liaoningotitan*, and it is in the transitional phase from early-diverging Titanosauriformes to late-diverging Titanosauriformes. The body type reconstruction of *Liaoningotitan*, which is referred to *Euhelopus zdanskyi*, shows that the *Liaoningotitan sinensis* holotype is more than 10 m long. Therefore, it is a medium-sized sauropod dinosaur. However, the unfused sacral vertebrae indicated the holotype is an immature specimen. In the end, we concluded the skull type of the Titanosauriformes. We got four types, indicating that the evolution of the Titanosauriformes may be more complex than we considered in the past.

ACKNOWLEDGEMENTS

Thanks to the Paleontological Museum of Liaoning (PMOL) of Shenyang Normal University for their research help, especially gratitude to Professor Hu Dongyu, Zhou Changfu, Xing Lida, Zhang Jianping, You Hailu, Sun Ge, Liu Yushuang, Liang Fei, Tian Ning, Li Li, Wu Sizhu, Zhang Xi, Zhang Yi, Zhao Mingsheng, Zhao Xin, Wang Li, museum staff, and my friends Sun Jingwen, Zhou Yue, Li Feifan, Yin Yalei, Gallipus and Hanging hand grenade (two net ID, they unwilling to announce their real name online) for their assistance, I spent a very beautiful time with them and look forward to continue collaborating with them in the future. In the end, I deeply mourn Professor Dong Zhiming, a great scientist, the one of the pioneers of Chinese Paleontology.

ADDITIONAL INFORMATION AND DECLARATIONS

Funding

The authors received no funding for this work.

Competing Interests

The authors declare that they have no competing interests.

Author Contributions

- Bingqing Shan conceived and designed the experiments, performed the experiments, analyzed the data, prepared figures and/or tables, authored or reviewed drafts of the article, and approved the final draft.

Data Availability

The following information was supplied regarding data availability:

A matrix of Titanosauriform dinosaurs is available at figshare: Shan, Bingqing (2024). Supplementary materials of the article ‘The re-description of *Liaoningotitan sinensis* Zhou *et al.*, 2018’ of Shan bingqing (author). figshare. Dataset. <https://doi.org/10.6084/m9.figshare.27964668.v4>.

Supplemental Information

Supplemental information for this article can be found online at <http://dx.doi.org/10.7717/peerj.19154#supplemental-information>.

REFERENCES

- Beeston SL, Poropat SF, Mannion PD, Pentland AH, Enchlmaier MJ, Sloan T, Elliott DA. 2024.** Reappraisal of sauropod dinosaur diversity in the Upper Cretaceous Winton Formation of Queensland, Australia, through 3D digitization and description of new specimens. *PeerJ* **12(6)**:e17180 DOI [10.7717/peerj.17180](https://doi.org/10.7717/peerj.17180).
- Borsuk-Bialynicka M. 1977.** A new camarasaurid sauropod *Opisthocoelicaudia skarzynskii* gen. n., sp. n. from the Upper Cretaceous of Mongolia. *Palaeontologia Polonica* **37**:5–63.
- Calvo JO. 2014.** New fossil remains of *Futalognkosaurus dukei* (Sauropoda, Titanosauria) from the Late Cretaceous of Neuquén, Argentina. In: Cerdeño E, ed. *4th International Palaeontological Congress. The History of Life: A View from the Southern Hemisphere Abstract Volume*. Washington, D.C.: International Palaeontological Association, 325.
- Carballido JL, Diego P, Alejandro O, Cerda IA, Salgado L, Garrido AC, Ramezani J, Cuneo NR, Krause JM. 2017.** A new giant titanosaur sheds light on body mass evolution among sauropod dinosaurs. *Proceedings of the Royal Society B: Biological Sciences* **284(1860)**:20171219 DOI [10.1098/rspb.2017.1219](https://doi.org/10.1098/rspb.2017.1219).
- D’Emic MD, Mannion PD, Upchurch P, Benson RBJ, Pang Q, Cheng Z. 2013.** Osteology of *Huabeisaurus allocotus* (Sauropoda: Titanosauriformes) from the Upper Cretaceous of China. *PLOS ONE* **8(8)**:e69375 DOI [10.1371/journal.pone.0069375](https://doi.org/10.1371/journal.pone.0069375).
- Daniel CB, Brooks BB, John AW, Wilson JA. 2010.** First complete sauropod dinosaur skull from the Cretaceous of the Americas and the evolution of sauropod dentition. *Naturwissenschaften* **97**:379–391 DOI [10.1007/s00114-010-0650-6](https://doi.org/10.1007/s00114-010-0650-6).
- Dong Z. 2001.** A forefoot of sauropod from the Tuchengzi Formation of Chaoyang area in Liaoning, China. In: *Proceeding of the English Annual Meeting of the Chinese Society of Vertebrate Paleontology*. Beijing: Ocean Press.
- Goloboff P, Catalano S. 2016.** TNT, version 1.5, with a full implementation of phylogenetic morphometrics. *Cladistics* **32(3)**:221–238 DOI [10.1111/cla.12160](https://doi.org/10.1111/cla.12160).
- Gomani EM. 2005.** Sauropod dinosaurs from The Early Cretaceous of Malawi, Africa. *Palaeontologia Electronica* **8(1)**:1–37.
- González Riga BJ, Lamanna MC, Ortiz David LD, Calvo JO, Coria JP. 2016.** A gigantic new dinosaur from the Argentina and the evolution of the Sauropod hind foot. *Scientific Reports* **6(1)**:6196 DOI [10.1038/srep19165](https://doi.org/10.1038/srep19165).
- Gorscak E, O’Connor PM. 2016.** Time-calibrated models support congruency between Cretaceous continental rifting and titanosaurian evolutionary history. *Biology Letters* **12(4)**:20151047 DOI [10.1098/rsbl.2015.1047](https://doi.org/10.1098/rsbl.2015.1047).
- Han F, Yang L, Lou F, Corwin S, Xu X, Qiu W, Liu H, Yu J, Wu R, Ke Y, Xu M, Hu J, Lu P. 2024.** A new titanosaurian sauropod, *Gandititan cavocaudatus* gen. et sp. nov., from the Late Cretaceous of southern China. *Journal of Systematic Palaeontology* **22(1)**:e2293038 DOI [10.1080/14772019.2023.2293038](https://doi.org/10.1080/14772019.2023.2293038).
- Huene VFF. 1932.** Die fossil Reptil-Ordnung Saurischia, ihre Entwicklung und Geschichte. *Monographien zur Geologie und Palaeontologie* **1(4)**:1–361.
- Lacovara K, Lamanna M, Ibiricu LM, Poole JC, Schroeter ER, Ullmann PV, Voegelé KK, Boles ZM, Carter AM, Fowler EK, Egerton VM, Moyer AE, Coughenour CL, Schein JP,**

- Jerald DHJD, Martínez RD, Novas FE. 2014.** A gigantic, exceptionally complete titanosaurian sauropod dinosaur from Southern Patagonia, Argentina. *Scientific Reports* **4**:6196 DOI [10.1038/srep06196](https://doi.org/10.1038/srep06196).
- Li L, Li D, You H, Dodsden P. 2014.** A new titanosauria sauropod from the Hekou Group (Lower Cretaceous) of the Lanzhou-Minhe Basin, Gansu Province, China. *PLOS ONE* **9**(1):e85979 DOI [10.1371/journal.pone.0085979](https://doi.org/10.1371/journal.pone.0085979).
- Li D, You H. 2009.** The first well-preserved Early Cretaceous Brachiosaurid dinosaur in Asia. *Proceedings of the Royal Society B Biological Science* **276**(1675):4077–4082 DOI [10.1098/rspb.2009.1278](https://doi.org/10.1098/rspb.2009.1278).
- Lü J, Azuma Y, Cheng R, Zheng W, Jin X. 2008.** A new titanosauriform sauropod from the Early Late Cretaceous of Dongyang Zhejiang Province. *Acta Geologica Sinica* **82**:225–235 DOI [10.1111/j.1755-6724.2008.tb00572.x](https://doi.org/10.1111/j.1755-6724.2008.tb00572.x).
- Lü J, Pu H, Xu L, Jia S, Zhang J, Shen C. 2014.** *Osteology of giant sauropod dinosaur Ruyangosaurus giganteus Lü et al.* Beijing: Geological Press.
- Lü J, Xu L, Jiang X, Jia S, Li M, Yuan C, Zhang X, Ji Q. 2009.** A preliminary report on the new dinosaurian fauna from the Cretaceous of the Ruyang Basin, Henan Province of central China. *Journal of the Paleontological Society of Korea* **25**(1):43–56.
- Lü J, Xu L, Zhang X, Pu H. 2007.** A new gigantic sauropod dinosaur with the deepest known body cavity from the cretaceous of Asia. *Acta Geologica Sinica* **81**(2):167–176 DOI [10.1111/j.1755-6724.2007.tb00941.x](https://doi.org/10.1111/j.1755-6724.2007.tb00941.x).
- Lü J, Xu L, Zhang X, Pu H, Zhang Y, Jia S, Chang H, Zhang J, Wei X. 2013a.** A new sauropod dinosaur (Dinosauria, Sauropoda) from the late Early Cretaceous of the Ruyang Basin (central China). *Cretaceous Research* **44**(3):202–213 DOI [10.1016/j.cretres.2013.04.009](https://doi.org/10.1016/j.cretres.2013.04.009).
- Lü J, Yi L, Zhong H, Wei X. 2013b.** A new somphospondylan sauropod (Dinosauria, Titanosauriformes) from the Late Cretaceous of Ganzhou, Jiangxi Province of Southern China. *Acta Geologica Sinica* **87**(3):678–685 DOI [10.1111/1755-6724.12079](https://doi.org/10.1111/1755-6724.12079).
- Mannion PD. 2011.** A reassessment of Mongolosaurus haplodont, Gilmore, 1933, a Titanosaurian sauropod dinosaur from the Early Cretaceous of Inner Mongolia, People's Republic of China. *Journal of Systematic Paleontology* **9**(3):355–378 DOI [10.1080/14772019.2010.527379](https://doi.org/10.1080/14772019.2010.527379).
- Mannion PD, Upchurch P, Barnes RN, Mateus O. 2013.** Osteology of the Late Jurassic Portuguese sauropod dinosaur *Lusotitan atalaiensis* (Macronaria) and the evolutionary history of basal titanosauriforms. *Zoological Journal of the Linnean Society* **168**(1):98–206 DOI [10.1111/zoj.12029](https://doi.org/10.1111/zoj.12029).
- Mannion PD, Upchurch P, Jin X, Zheng W. 2019a.** New information on the Cretaceous sauropod dinosaurs of Zhejiang Province China: impact on Laurasian Titanosauriformes phylogeny and biogeography. *Royal Society Open Science* **6**(8):1–22 DOI [10.1098/rsos.191057](https://doi.org/10.1098/rsos.191057).
- Mannion PD, Upchurch P, Schwarz D, Wings O. 2019b.** Taxonomic affinities of the putative titanosaurs from the Late Jurassic Tendaguru Formation of Tanzania: phylogenetic and biogeographic implications for eusauropod dinosaur evolution. *Zoological Journal of Linnean Society* **185**:784–905 DOI [10.1093/zoolinlean/zly068](https://doi.org/10.1093/zoolinlean/zly068).
- Marsh OC. 1878.** Principal characters of American Jurassic dinosaurs. Pt. I. *American Journal of Science (Series 3)* **16**(95):411–416 DOI [10.2475/ajs.s3-16.95.411](https://doi.org/10.2475/ajs.s3-16.95.411).
- Martinez RD, Lamanna MC, Novas FE, Ridgely CR, Casal GA, Martínez JE, Vita JR, Witmer LM. 2016.** A basal lithostrotian titanosaur (Dinosauria: Sauropoda) with a complete skull: implications for the evolution and paleobiology of Titanosauria. *PLOS ONE* **11**(4):e0151661 DOI [10.1371/journal.pone.0151661](https://doi.org/10.1371/journal.pone.0151661).

- Mo J. 2013.** *Bellusaurus sui*. *Topics in Chinese dinosaurs paleontology*. Zhengzhou: Henan Scientific and Technical Press, 1–155.
- Mo J, Fu Q, Yu Y, Xu X. 2023.** A new titanosaurian sauropod from the Upper Cretaceous of Jiangxi Province, Southern China. *Historical Biology* **36(11)**:2443–2457
DOI [10.1080/08912963.2023.2259413](https://doi.org/10.1080/08912963.2023.2259413).
- Mo J, Huang C, Zhao Z, Wang Xu, X. 2008.** A new titanosauria (Dinosauria: Sauropoda) from the Late Cretaceous of Guangxi China. *Vertebrata Palasiactia* **46**:147–156.
- Mo J, Li J, Ling Y, Buffetaut E, Suteethorn S, Varavudh S, Tong HY, Gilles CG, Romain AG, Xu X. 2020.** New fossil remains of *Fusuisaurus zhaoi* (Sauropoda: Titanosauriformes) from the Lower Cretaceous of Guangxi China. *Cretaceous Research* **109(5)**:104379
DOI [10.1016/j.cretres.2020.104379](https://doi.org/10.1016/j.cretres.2020.104379).
- Mo J, Ma F, Yu Y, Xu X. 2022.** A new titanosauriform sauropod with an unusual tail from the Lower Cretaceous of Northeastern China. *Cretaceous Research* **144(1860)**:105449
DOI [10.1016/j.cretres.2022.105449](https://doi.org/10.1016/j.cretres.2022.105449).
- Mo J, Wang K, Wang P, Chen S, Xu X. 2017.** A new titanosauria dinosaur from Late Cretaceous of Shandong. *Geological Bulletin of China* **36(9)**:1501–1505.
- Mo J, Wang W, Huang Z, Huang X, Xu X. 2006.** A basal Titanosauriform from the Guangxi. *China Acta Geologica Sinica* **80(4)**:486–489.
- Mo J, Xu X, Buffetaut E. 2010.** A new eusauropod dinosaur from the Lower Cretaceous of Guangxi Province, Southern China. *Acta Geologica Sinica* **84**:1328–1335
DOI [10.1111/j.1755-6724.2010.00331.x](https://doi.org/10.1111/j.1755-6724.2010.00331.x).
- Otero A, Carballido JL, Moreno PA. 2020.** The appendicular osteology of *Patagotitan mayorum* (Dinosauria, Sauropoda). *Journal of Vertebrate Paleontology* **40(4)**:1–20
DOI [10.1080/02724634.2020.1793158](https://doi.org/10.1080/02724634.2020.1793158).
- Ouyang H. 2003.** *Skeletal characteristics of Mamenchisaurus youngi and the systematics of Mamenchisaurids*. Chengdu: Chengdu Technical University, 1–176.
- Pang Q, Cheng Z. 2000.** A new sauropod dinosaur from the Late Cretaceous of Tianzhen Shanxi Province China. *Acta Geologica Sinica* **74**:2–9.
- Paul GS. 1988.** The brachiosaur giants of the Morrison and Tendaguru with a description of a new subgenus, *Giraffatitan*, and a comparison of the world's largest dinosaurs. *Hunteria Societas Paleontographica Goloradensis* **2(3)**:1–14.
- Poropat SF, Benjamin PK. 2013.** Photographic Atlas and three-dimensional reconstruction of the holotype skull of *Euhelopus zdanskyi* with description of additional cranial elements. *PLOS ONE* **8(11)**:e79932 DOI [10.1371/journal.pone.0079932](https://doi.org/10.1371/journal.pone.0079932).
- Poropat SF, Mannion PD, Rigby SL, Ducan RJ, Pentland AH, Bevitt JJ, Sloan T, Elliott DA. 2023.** A nearly complete skull of the sauropod dinosaur *Diamantinasaurus matildae* from the Upper Cretaceous Winton Formation of Australia and implications for the early evolution of titanosaurs. *Royal Society Open Science* **10(4)**:221618 DOI [10.1098/rsos.221618](https://doi.org/10.1098/rsos.221618).
- Poropat SF, Upchurch P, Mannion PD, Hocknull SA, Benjamin PK, Trish S, George HKS, Elliott D. 2014.** Revision of the sauropod dinosaur *Diamantinasaurus matildae* Hocknull et al. 2009 from the mid-Cretaceous of Australia: implications for Gondwanan titanosauriform dispersal. *Gondwana Research* **27(2015)**:995–1033 DOI [10.1016/j.gr.2014.03.014](https://doi.org/10.1016/j.gr.2014.03.014).
- Ren X. 2020.** *Early evolution of sauropod dinosaurs based on new discovery and restudy of Chinese Middle Jurassic specimens*. Beijing: University of Chinese Academic Science, 1–295.
- Ren X, Jiang S, Wang X, Peng G, Ye Y, King L, You H. 2022.** Osteology of *Dashanpusaurus dongi* (Sauropoda: Macronaria) and new evolutionary evidence from Middle Jurassic Chinese

- sauropods. *Journal of Systematic Palaeontology* **20**(1):2132886
DOI [10.1080/14772019.2022.2132886](https://doi.org/10.1080/14772019.2022.2132886).
- Rogers KC. 2009.** The postcranial osteology of *Rapetosaurus krausei* (Sauropoda: Titanosauria) from the Late Cretaceous of Madagascar. *Journal of Vertebrate Paleontology* **29**(4):1046–1086
DOI [10.1671/039.029.0432](https://doi.org/10.1671/039.029.0432).
- Rogers KC, Forster RCA. 2004.** The skull of *Rapetosaurus krausei* (Sauropoda: Titanosauria) from the Late Cretaceous of Madagascar. *The Society of Vertebrate Paleontology* **24**(1):121–144
DOI [10.1671/A1109-10](https://doi.org/10.1671/A1109-10).
- Salgado L, Coria RA, Calvo JO. 1997.** Evolution of titanosaurid sauropods I: phylogenetic analysis based on the postcranial evidence. *Ameghiniana* **34**:3–32.
- Seeley HG. 1887.** On the classification of the fossil animals commonly named Dinosauria. *Proceedings of the Royal Society of London* **43**:165–171 DOI [10.1098/rspl.1887.0117](https://doi.org/10.1098/rspl.1887.0117).
- Smith JB, Lammana MC, Lacovara KJ, Dodson P, Smith JR, Poole JC, Giegengack R, Attia Y. 2001.** A giant sauropod dinosaur from an Upper Cretaceous Mangrove deposit in Egypt. *Science* **292**(5522):1704–1706 DOI [10.1126/science.1060561](https://doi.org/10.1126/science.1060561).
- Tang F, Jin X, Kang X, Zhang G. 2001.** *Omeisaurus maoianus* A complete Sauropoda from Jingyan, Sichuan. Beijing: Ocean Press.
- Wang X, Bandeira KLN, Qiu R, Jiang S, Cheng X, Ma YX, Kellner AWA. 2021.** The first dinosaurs from the Early Cretaceous Hami Pterosaur Fauna, China. *Scientific Reports* **11**:14962
DOI [10.1038/s41598-021-94273-7](https://doi.org/10.1038/s41598-021-94273-7).
- Wang X, Wu W, Li T, Ji Q, Li Y, Guo J. 2019.** A new titanosauriform dinosaur (Dinosauria: Sauropoda) from Late Jurassic of Junggar Basin, Xinjiang. *World Geology* **38**(3):581–588
DOI [10.3969/j.issn.1004-5589.2019.03.001](https://doi.org/10.3969/j.issn.1004-5589.2019.03.001).
- Wang X, You H, Gao C, Cheng X, Liu J. 2007.** *Dongbeititan dongi* the first sauropod dinosaur from the Lower Cretaceous Jehol Group of Western Liaoning Province China. *Acta Geologica Sinica* **6**:911–916 DOI [10.1111/j.1755-6724.2007.tb01013.x](https://doi.org/10.1111/j.1755-6724.2007.tb01013.x).
- Wilson JA. 2005.** Redescription of Mongolia sauropod *Nemegtosaurus mongoliensis* Nowinskyi (Dinosauria: Saurichia) and comments on Late Cretaceous Sauropod diversity. *Journal of Systematic Paleontology* **3**:283–318.
- Wilson JA, Diego P, Carvalho AB, Hussam Z. 2016.** The skull of the Titanosaur *Tapuiasaurus macedoi* (Dinosauria: Sauropoda) a basal titanosaur from the lower Cretaceous of Brazil. *Zoological Journal of Linnean Society* **178**:611–662 DOI [10.1111/zoj.12420](https://doi.org/10.1111/zoj.12420).
- Wilson JA, Sereno P. 1998.** Early evolution and higher-level phylogeny of sauropod dinosaurs. *Society of Vertebrate Paleontology* **18**:1–79 DOI [10.1080/02724634.1998.10011115](https://doi.org/10.1080/02724634.1998.10011115).
- Wilson JA, Upchurch P. 2009.** Redescription and reassessment of the phylogenetic affinities of the *Euhelopus zdanskyi* (Dinosauria: Sauropoda) from the Early Cretaceous of China. *Journal of Systematic Paleontology* **7**(2):199–239 DOI [10.1017/S1477201908002691](https://doi.org/10.1017/S1477201908002691).
- Wu W. 2006.** *A new sauropod dinosaur (Jiutaisaurus) from Cretaceous in Jiutai of Jilin, China.* Changchun: Jilin University, 1–41.
- Xu X, You H, Mo J. 2021.** *Palaeovertebrata sinica, volume II: amphibians, reptiles, and avians: fascicle 6 (Serial no.10): Saurischian Dinosaurs.* Beijing: Science Press.
- Xu X, Zhang X, Tan Q, Zhao X, Tan L. 2006.** A new titanosaurian from Late Cretaceous of Nei Mongol, China. *Acta Geologica Sinica* **80**(1):20–26 DOI [10.1111/j.1755-6724.2006.tb00790.x](https://doi.org/10.1111/j.1755-6724.2006.tb00790.x).
- Xue X, Zhang Y, Bi Y, Yue L, Chen D. 1996.** *The development and environmental changes of the intermontane basins in the Eastern Part of Qinling Mountains.* Beijing: Geological Press.

- Yang C. 2014.** *The phylogenetic evolution of Mamenchisauridae*. Chengdu: Chengdu Technical University, 1–172.
- You H, Ji Q, Lamanna MC, Li J, Li Y. 2004.** A titanosaurian sauropod dinosaur with opisthocoelous caudal vertebrae from the Early Late Cretaceous of Liaoning Province, China. *Acta Geologica Sinica* **78**(4):907–911 DOI [10.1111/j.1755-6724.2004.tb00212.x](https://doi.org/10.1111/j.1755-6724.2004.tb00212.x).
- You H, Li D, Zhou L, Ji Q. 2006.** *Huanghetitan liujiaxiaensis*: a new sauropod dinosaur from Hekou Group of Lower Cretaceous in Lanzhou Basin Gansu China. *Geological Review* **52**:669–674.
- You H, Li D, Zhou L, Ji Q. 2008.** *Daxiatitan binglingi*: a giant sauropod dinosaur from The Early Cretaceous of China. *Gansu Geology* **17**:2–10.
- You H, Tang F, Luo Z. 2003.** A new basal titanosaur (Dinosauria: Sauropoda) from the Early Cretaceous of China. *Acta Geologica Sinica* **77**(4):424–429 DOI [10.1111/j.1755-6724.2003.tb00123.x](https://doi.org/10.1111/j.1755-6724.2003.tb00123.x).
- Zhang Y. 1988.** *The middle Jurassic dinosaur fauna from Dashanpu Zigong Sichuan: Sauropod Dinosaurs (I): Shunosaurus*. Chengdu: Sichuan Technological Press.
- Zhang L. 2020.** Analysis on fossil community of tetrapods in Lujiatun bed of Lower Cretaceous Yixian Formation in Beipiao, Liaoning. *Global Geology* **39**:738–744 DOI [10.3969/j.issn.1004-5589.2020.04.001](https://doi.org/10.3969/j.issn.1004-5589.2020.04.001).
- Zhang X, Lü J, Xu L, Li J, Yang L, Hu W, Jia S, Ji Q, Zhang C. 2009.** A new sauropod dinosaur from the Late Cretaceous Gaogou Formation of Nanyang, Henan Province. *Acta Geologica Sinica* **83**(2):212–221 DOI [10.1111/j.1755-6724.2009.00032.x](https://doi.org/10.1111/j.1755-6724.2009.00032.x).
- Zhou C, Wu W, Toru S, Dong Z. 2018.** A new titanosauriformes dinosaur from Jehol Biota of western Liaoning China. *Global Geology* **37**:328–333.